The Thesis Committee for Han Kang
certifies that this is the approved version of the following thesis:

Forecasting Congestion in Transmission Line and Voltage Stability with Wind Integration

Committee:

Baldick, Ross, Supervisor

Grady, W. Mack

Forecasting Congestion in Transmission Line and Voltage Stability with Wind Integration

by

Han Kang, B.S.

THESIS

Presented to the Faculty of the Graduate School of

The University of Texas at Austin

in Partial Fulfillment

of the Requirements

for the Degree of

MASTER OF SCIENCE IN ENGINEERING

THE UNIVERSITY OF TEXAS AT AUSTIN

August 2011

Dedicated to my parents and sister.

Acknowledgments

This work has been carried out at the Division of Energy System Track, Department of Electrical and Computer Engineering at The University of Texas at Austin.

First and foremost, I would like to express my deep and sincere appreciation to my supervisor Dr. Ross Baldick for his excellent supervision during the work as well as giving the opportunity for me to study in depth the area of power system.

I would like to express my gratitude to my senior student, Jin Hur and for his enthusiastic care of this work. My gratitude also goes to all the Korean students at Energy System Track for providing excellent advices.

Also thanks a lot to those people I met who helped me in different ways without being aware of that.

Naturally, the most heartfelt thanks to my parents, Kwangil Kang and Chunkok Kim to support me both materially and morally every day that I was far away from them.

Last but not least, I also would like to thank my old friends Sungin Cho, Dongun Sohn, Woongjin Byun, and Inwoo Nam.

Forecasting Congestion in Transmission Line and Voltage Stability with Wind Integration

Han Kang, M.S.E.
The University of Texas at Austin, 2011

Supervisor: Baldick, Ross

Abstract

Due to growth of wind power, system operators are being challenged by the integration of large wind farms into their electrical power systems. Large scale wind farm integration has adverse effects on the power system due to its variable characteristic. These effects include two main aspects: voltage stability and active line flow. In this thesis, a novel techniques to forecast active line flow and select pilot bus are introduced with wind power integration.

First, this thesis introduces a methodology to forecast congestion in the transmission line with high wind penetration. Since most wind resources tend to be located far away form the load center, the active line flow is one of the most significant aspects when wind farm is connected to electrical grid. By providing the information about the line flow which can contribute to transmission line congestion, the system operators would be able to respond such as by requesting wind power or load reduction.

The second objective of this thesis is to select the weakest bus, called pilot bus, among all load buses. System reliability, especially voltage stability, can be adversely affected by wind variability. In order to ensure reliable operation of power systems with wind power integration, the index to select the pilot bus is developed, and further prediction of voltage profile at the pilot bus is fulfilled. The objective function to select the pilot bus takes account of the N-1 contingency analysis, loading margin, and reactive power sensitivity. Through on the objective function, the pilot bus is representative of all load buses as well as controllable by reactive power regulation. Predicting the voltage profile at the pilot bus is also useful for system operators to determine wind power output.

Table of Contents

List of Tables

List of Figures

Chapter 1

Introduction

1.1 Background

For many years, the effort to reduce emissions from conventional power plants continues to increase throughout the world. Renewable resources come into the spotlight as one of the solutions. However, there still exist problems of the integration of renewable energy into the existing electrical grid due to its intermittent characteristics. In order to solve such problems, transmission system operators continue to make various efforts.

According to the year 2010 statistic report of the World Wind Energy Association (WWEA), the amount of installed wind turbines has undergone rapid increase worldwide. Worldwide installed wind capacity is 196,630 Megawatt, and 37,642 Megawatt of wind turbines were installed in 2010, somewhat less than in 2009. All wind turbines installed by the end of 2010 worldwide can generate 430 Terawatt hours per annum, which is more than the total electricity demand of the United Kingdom, the sixth largest economy of the world, and are approximately 2.5% of the global electricity consumption. The trend of the growth of wind generation worldwide is shown in Figure 1.1 [3]. Especially five countries –China, United States, Germany, Spain and India – have more than 75% of worldwide wind energy capacity [4].

Consequently, in order to utilize the installed wind power efficiently,

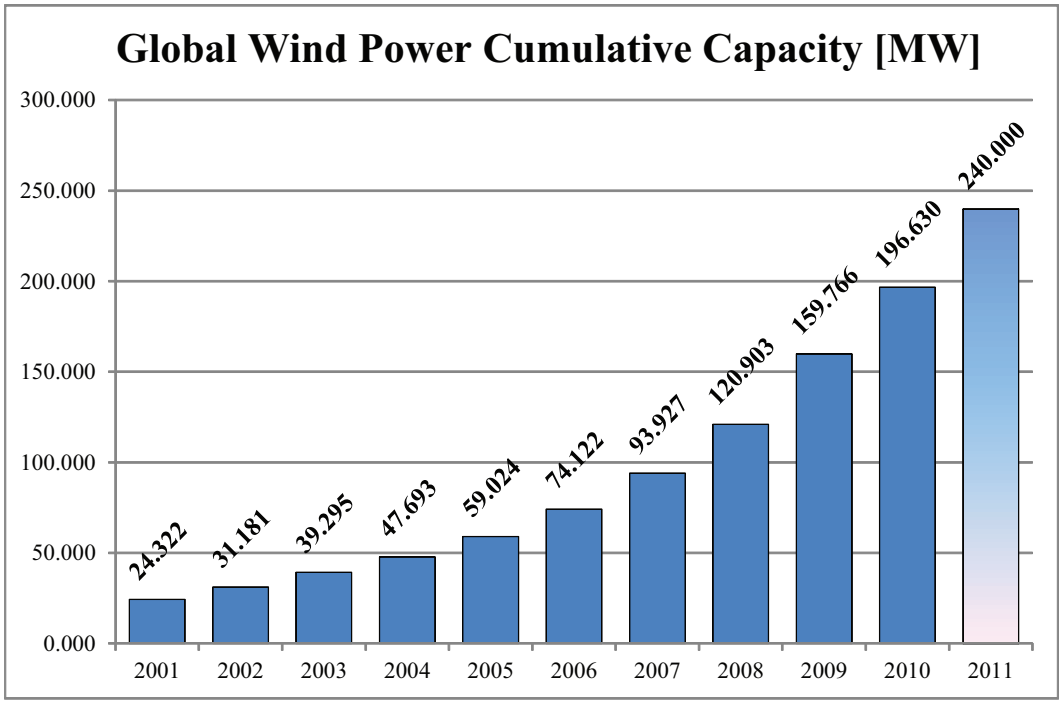

Figure 1.1: Wind Power World Total Installed Capacity [3]

numerous researches related to wind power have been conducted globally. The researches specifically focus on the issues related to wind energy generation and its integration into the power systems since the wind power presents additional huge uncertainties for the power system operation. In spite of the efforts, there are several problems still remaining with respect to integration, such as transmission line expansion, wind forecasting, market scheduling intervals, integration costs, and operating reserves [30].

To be specific, integrating large scale wind farm into an existing electrical grid is problematic due to congestion in transmission lines as well as voltage

stability because of the variability. The transmission lines have more possibilities to be congested by large scale wind farm integration. One of the reasons is that the most of good wind resources are located far from the load centers, but the capacities of installed transmission lines are limited. Moreover, it is costly and time-consuming to site and build more transmission lines. Another aspect is that the integration makes harmful effects on the voltage stability of transmission network as the wind penetration level increase, because of the intermittent generation. Therefore, independent system operators should have capability to manage not only the voltage stability, but also line constraints with wind uncertainties [13].

1.2 Contribution of the Thesis

The objective of the research is to develop forecasting short-term transmission line flow and selecting pilot bus in transmission network with high wind penetration. By providing the information of forecasted congestion in transmission lines and voltage profile at the chosen pilot bus, system operators will be able to prepare the remedial actions such as requested load reduction or redispatch of the existing generators [34].

In the thesis, an algorithm is proposed to develop forecasts of possible congested lines with high wind penetration. System operators are required to predict when and where they will need to take emergency actions to deal with a bottleneck in transmission line. Furthermore, it can be used to measure different power generation scenarios. By obtained system data of scheduled

generation and forecasted load and wind, the proposed method is utilized to predict active power flow in the lines with high probability of congestion. Especially, in the case of summer peak, it would be more helpful for grid operators to prevent and solve power crisis [1, 21, 26].

Secondly, the index is developed to select a pilot bus. In this work, a novel technique is proposed to identify the weakest bus in certain area, namely "Pilot Bus". The pilot bus is required to be representative and controllable throughout entire power system. This objective is achieved by use of N-1 contingency analysis and sensitivity analysis of whole power grid [25]. The variation of voltage at the pilot bus is a useful index of voltage stability of the entire system as well as being readily controllable by a relatively small amount of reactive power.

As the bottleneck and voltage stability in transmission network can be forecasted short-term, the system operators will be able to predict the time and location that the system will be unreliable. It is beneficial to prevent transmission line congestion and voltage collapse resulting from the high wind penetration by preparing a remedial action determine wind penetration level.

1.3 Outline of the Thesis

This thesis is organized as follow:

In chapter 1, brief introduction and contribution of the thesis are presented about the work done in the thesis. In chapter 2, previous works related to wind power, congestion forecasting, system reliability and pilot bus selec-

tion are summarized. In chapter 3, a proposed method to forecast congestion based on sensitivity analysis with the integration of wind power is introduced. In chapter 4, a novel approach for pilot bus selection is discussed. This technique takes N-1 contingency analysis and sensitivity analysis into account. In chapter 5, results of case studies of proposed methods in this thesis with two IEEE test system are presented. In chapter 6, the conclusion of the thesis and possible future work are discussed.

Chapter 2

Literature Survey

2.1 Introduction

In view of the worldwide increase of wind generation, it is becoming more difficult for the system operators to maintain reliability of power system under increasing uncertainty. Voltage stability and transmission line congestion are important factors in determining wind penetration level for reliable operation of electric grids. In order to operate the entire network reliably, the flow of active power through transmission line should not exceed the thermal limit of the line, and the voltage should avoid to be collapsed under an acceptable voltage level. In this chapter, a brief outline of the issues of transmission line congestion and voltage stability with wind power and other previous works in these areas are presented.

2.2 Wind Power

In recent ten years, from 2000 to 2010, wind energy has undergone rapid growth reaching approximately 196,630 MW of nameplate capacity installed worldwide at the end of 2010. It has played a significant role as one of the dominant resources amongst new capacity on many electric utility systems

[3]. The United States is also experiencing major changes with the growth of wind power development. As the country with the second largest wind capacity after China, the installed wind capacity in United States grew from 2,539 MW to 40,180 MW in 10 years. This rapid increase was stimulated especially by nationwide policies such as Production Tax Credit (PTC) and State Renewable Portfolio Standards (RPS) [33].

2.2.1 Wind Power Integration

Due to the steep increase, integration of the wind power into electrical grid presents a variety of difficulties for system operators. The main reason for these difficulties is derived from intermittent characteristics of wind power generation, which may result in unreliability of transmission network. Thus, in order to overcome these difficulties, the operators have performed a wide variety of studies of technical and economic impacts of incorporating wind plants into their system. Reference [33] introduces a wealth of information on the expected impacts of wind plants on power system operation and planning and provides valuable insights into possible strategies for dealing with them.

Nowadays, the system operators may require modification of existing power system and change of operation approaches according to the increasing integration of wind power into the system. Wind power integration makes adverse impacts on the system because the power system was not originally designed to accommodate this form of resource and the impacts come from the non-dispatchable nature of wind power[35]. These challenges can be broken

down into components associated with variability and uncertainty [13]. In order to reliably supply electricity from wind power to customers through the network, two main aspects should be taken into account. The first is to keep an acceptable voltage level to avoid voltage collapse and the other is to maintain the power balance of the system [4]. Accordingly, a wide variety of studies concerning wind integration are conducted in association with voltage stability and power balance.

2.3 Review of Congestion Forecasting

When transmission facilities are limited in delivering energy to some loads, transmission congestion occurs [2]. Transmission congestion makes adverse impacts not only on the system reliability but also on the price of energy. Thus, long-term and short-term planning of transmission and resource play significant role in preventing congestion [29].

Recent congestion forecasting studies focus on two categories of techniques. One is the extension of electricity price forecasting to congestion forecasting [8, 20] and the other is adoption of probabilistic approach to study the load flow problem [6, 9, 29].

2.4 Review of Basic System Stability

Power system stability is based on fundamental mathematics, analogous to the stability of any dynamic system. In [23], the power system stability refers to "the ability of an electric power system, for a given initial operating

condition, to regain a state of operating equilibrium after being subjected to a physical disturbance, with most system variables bounded so that practically the entire system remains intact."

The power system is a highly nonlinear system that is subject to constantly changing environments such as loads and generators output. Additionally, the power system can be affected by a wide range of disturbances, small and large. In order to efficiently manage a wide variety of stability issues, generally the power system stability is categorized as shown in Figure 2.1.

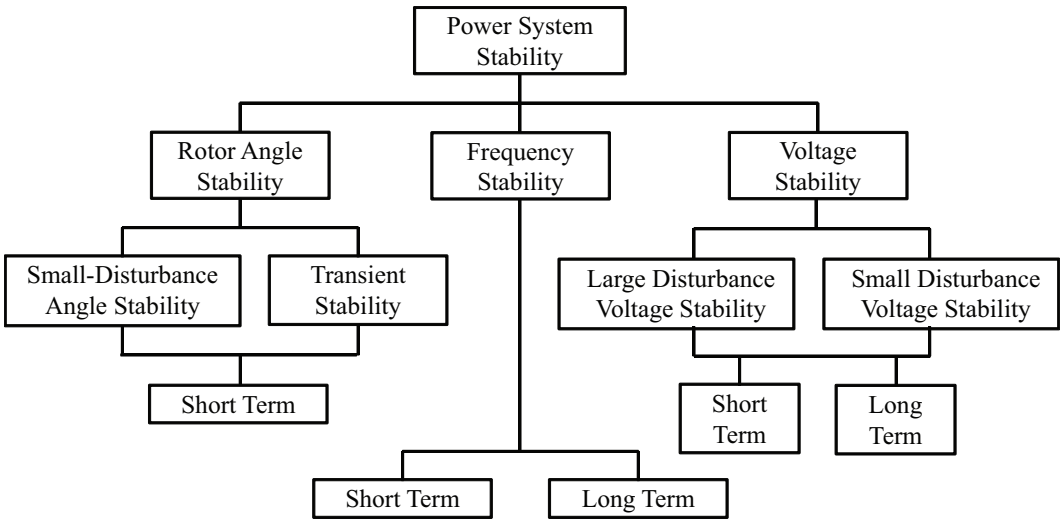

Figure 2.1: Classification of power system stability

2.4.1 Voltage Stability

As one of the aspects of system stability, voltage stability is important to maintain and restore equilibrium between load demand and supply. For stable operation of the system, the voltage level in the transmission system

should be kept at a technical and economical optimum by adjusting the reactive power [23]. Instability may bring out adverse impacts to the system, such as load shedding, tripping of transmission lines and other elements, and further cascading outages. One important concept related to voltage stability is voltage collapse, which can occur as the final outcome of voltage instability. The voltage collapse is a sudden and catastrophic phenomenon, which is brought out by heavily loading conditions. To avoid the voltage instability during disturbances, reactive reserves should be allocated throughout the system to maintain the voltage level [16].

2.4.2 Voltage Control

Voltage control is performed to secure acceptable voltage levels at every bus in transmission network by reactive power regulation. The voltage control is organized into three hierarchical levels, which are primary, secondary and tertiary.

- **Primary control level** : Rapid and random voltage deviation is the object to be controlled by the controllers of the primary control level such as a generator Automatic Voltage Regulator (AVR). The main objective is to keep their voltage level close to the desired reference values.

- **Secondary control level** : This control level manages slow and large voltage variations. Through keeping voltages of the pilot buses at their reference values by the control of primary control level, it is possible

to maintain the appropriate voltage profile throughout the transmission network. European countries especially take advantage of the secondary voltage control to improve voltage security and operation throughout the entire network [14, 15, 24, 31]

- **Tertiary control level** : In order to achieve economic and secure operation of the network, this control system is designed to utilize system-wide information. This control level deals with much slower variation of voltage than secondary voltage level with respect to the idea of coordination [12].

2.4.3 Pilot Bus Selection

In general, a pilot bus is defined as a bus which is chosen such that its voltage variation is representative of the voltage evolution throughout a given zone [24]. For the pilot bus selection, in [24], the pilot bus is chosen as the most central bus identified by electrical distance of the system and the paper shows how to calculate the electrical distance. In [31], the bus which has the greatest short circuit capacity among all load buses is selected as the pilot bus. Conejo, et al. introduces the method to select the pilot bus by nonlinear approach using the full load flow equation [12].

Most importantly, the pilot bus selection is required to satisfy two important criteria, observability and controllability [31]. In other words, voltage at the pilot bus should be representative of voltage at all buses, and readily controllable by generators and any other devices for supporting reactive power.

Chapter 3

Congestion Forecasting with Wind Integration

3.1 Introduction

In this chapter, an innovative technique is developed using sensitivity analysis for forecasting congestion in a selected critical line with wind integration. Transmission line congestion makes adverse impacts on electrical grid operation such as load curtailment. Additional uncertainty from installed wind farm may result in higher probability of congestion, because the fluctuation of wind power increases uncertainty in the transmission power flow. Additionally, grouped wind farms are located far away from the load centers [36]. Therefore, information about specific location and time of potential congestion will be highly helpful for system operators to prepare remedial action such as request for load or wind generation reduction [26].

3.2 Line Flow Formulation

For node l in the transmission network, active power and reactive power injection can be calculated from (3.1) and (3.2).

$$P_l = \sum u_l u_k \left[G_{lk} \cos(\theta_l - \theta_k) + B_{lk} \sin\left(\theta_l - \theta_k\right) \right] \tag{3.1}$$

$$Q_l = \sum u_l u_k \left[G_{lk} \sin(\theta_l - \theta_k) - B_{lk} \cos\left(\theta_l - \theta_k\right) \right] \tag{3.2}$$

where u_l and u_k are voltage magnitudes at the bus l and k respectively, θ_l and θ_k are voltage angle at bus l and k respectively, and G_{lk} and B_{lk} are conductance and susceptance respectively of the transmission line between bus l and k.

In order to apply the Newton-Raphson method to solve this nonlinear equation, (3.1) and (3.2) are linearized as (3.3).

$$\begin{bmatrix} \boldsymbol{\theta} \\ \mathbf{V} \end{bmatrix} = \begin{bmatrix} \dfrac{\partial \mathbf{P}}{\partial \boldsymbol{\theta}} & \dfrac{\partial \mathbf{P}}{\partial \mathbf{V}} \\ \dfrac{\partial \mathbf{Q}}{\partial \boldsymbol{\theta}} & \dfrac{\partial \mathbf{Q}}{\partial \mathbf{V}} \end{bmatrix}^{-1} \begin{bmatrix} \mathbf{P}_{\text{inj}} \\ \mathbf{Q}_{\text{inj}} \end{bmatrix} \tag{3.3}$$

Once the voltage magnitude and the angle at each bus are specified, the active power and reactive power flow between two nodes, node l and k, can be calculated from (3.4) and (3.5).

$$P_{lk} = u_l u_k \left[G_{lk} \cos\left(\theta_l - \theta_k\right) + B_{lk} \sin\left(\theta_l - \theta_k\right) \right] - (u_l)^2 G_{lk} \tag{3.4}$$

$$Q_{lk} = u_l u_k \left[G_{lk} \sin\left(\theta_l - \theta_k\right) - B_{lk} \cos\left(\theta_l - \theta_k\right) \right] + (u_l)^2 B_{lk} \tag{3.5}$$

The function of active and reactive power flow can be expressed as (3.6) and (3.7).

$$\mathbf{P}_{\text{line}} = \mathbf{F}\mathbf{P}_{\text{flow}}\left(\mathbf{V}, \boldsymbol{\theta}\right) \tag{3.6}$$

$$\mathbf{Q}_{\text{line}}=\mathbf{FQ}_{\text{flow}}\left(\mathbf{V},\boldsymbol{\theta}\right) \tag{3.7}$$

where $\mathbf{P}_{\text{line}}$ is a vector of the active line flows, $\mathbf{V}$ is a vector of the voltage magnitude, $\boldsymbol{\theta}$ is a vector of the voltage angle, and $\mathbf{FP}_{\text{flow}}$ and $\mathbf{FQ}_{\text{flow}}$ is a vector of functions for active and reactive power line flow, respectively as shown in (3.4) and (3.5).

By linearizing (3.6), the active and reactive line flow can be expressed with a function of active and reactive power injections as shown in (3.8).

$$\begin{bmatrix} \mathbf{P}_{\text{line}} \\ \mathbf{Q}_{\text{line}} \end{bmatrix} = \begin{bmatrix} \frac{\partial \mathbf{FP}_{\text{flow}}}{\partial \boldsymbol{\theta}} & \frac{\partial \mathbf{FP}_{\text{flow}}}{\partial \mathbf{V}} \\ \frac{\partial \mathbf{FQ}_{\text{flow}}}{\partial \boldsymbol{\theta}} & \frac{\partial \mathbf{FQ}_{\text{flow}}}{\partial \mathbf{V}} \end{bmatrix} \begin{bmatrix} \frac{\partial \mathbf{P}}{\partial \boldsymbol{\theta}} & \frac{\partial \mathbf{P}}{\partial \mathbf{V}} \\ \frac{\partial \mathbf{Q}}{\partial \boldsymbol{\theta}} & \frac{\partial \mathbf{Q}}{\partial \mathbf{V}} \end{bmatrix}^{-1} \begin{bmatrix} \mathbf{P}_{\text{inj}} \\ \mathbf{Q}_{\text{inj}} \end{bmatrix} \tag{3.8}$$

To estimate the change of active power line flow between two time frames, (3.8) can be converted to the form of (3.9).

$$\begin{bmatrix} \Delta\mathbf{P}_{\text{line}}(t) \\ \Delta\mathbf{Q}_{\text{line}}(t) \end{bmatrix} = \begin{bmatrix} \mathbf{P}_{\text{line}}(t0) \\ \mathbf{Q}_{\text{line}}(t0) \end{bmatrix} + \begin{bmatrix} \frac{\partial \mathbf{FP}_{\text{flow}}}{\partial \boldsymbol{\theta}} & \frac{\partial \mathbf{FP}_{\text{flow}}}{\partial \mathbf{V}} \\ \frac{\partial \mathbf{FQ}_{\text{flow}}}{\partial \boldsymbol{\theta}} & \frac{\partial \mathbf{FQ}_{\text{flow}}}{\partial \mathbf{V}} \end{bmatrix} \begin{bmatrix} \frac{\partial \mathbf{P}}{\partial \boldsymbol{\theta}} & \frac{\partial \mathbf{P}}{\partial \mathbf{V}} \\ \frac{\partial \mathbf{Q}}{\partial \boldsymbol{\theta}} & \frac{\partial \mathbf{Q}}{\partial \mathbf{V}} \end{bmatrix}^{-1} \begin{bmatrix} \Delta\mathbf{P}_{\text{inj}} \\ \Delta\mathbf{Q}_{\text{inj}} \end{bmatrix} \tag{3.9}$$

3.3 Congestion Forecasting Procedure

Figure 3.1 represents the flowchart of congestion forecasting procedure. Description of each part is as follows step by step.

3.3.1 System Data Acquisition

The main objective of this step is to obtain the system data. The system data primarily includes information about the power system such as generator, load and transmission line.

- Generator information : P_{Gmax}, P_{Gmin}, Q_{Gmax}, and Q_{Gmin}
- Load information : P_L and Q_L
- Transmission Line information : $R_{jk} + iG_{jk}$ and $P_{jk,\text{lim}}$

3.3.2 Pre-contingency Sensitivity Calculation

From the obtained system information, the pre-contingency sensitivity can be formulated as (3.10) from (3.9).

$$\alpha = \begin{bmatrix} \frac{\partial \mathbf{FP}_{\text{flow}}}{\partial \boldsymbol{\theta}} & \frac{\partial \mathbf{FP}_{\text{flow}}}{\partial \mathbf{V}} \\ \frac{\partial \mathbf{FQ}_{\text{flow}}}{\partial \boldsymbol{\theta}} & \frac{\partial \mathbf{FQ}_{\text{flow}}}{\partial \mathbf{V}} \end{bmatrix} \begin{bmatrix} \frac{\partial \mathbf{P}}{\partial \boldsymbol{\theta}} & \frac{\partial \mathbf{P}}{\partial \mathbf{V}} \\ \frac{\partial \mathbf{Q}}{\partial \boldsymbol{\theta}} & \frac{\partial \mathbf{Q}}{\partial \mathbf{V}} \end{bmatrix}^{-1} \tag{3.10}$$

3.3.3 Post-contingency Sensitivity Calculation

When contingency occurs, the sensitivity matrix changes since line impedance values would be varied. For evaluating post-contingency case, the post-contingency sensitivity matrix can be obtained from (3.11). Since Every contingency has a different matrix, this equation needs to be calculated as the

number of contingencies.

$$\beta_{jk}= \begin{bmatrix} \dfrac{\partial \mathbf{FP}_{\text{flow},jk}}{\partial \boldsymbol{\theta}} & \dfrac{\partial \mathbf{FP}_{\text{flow},jk}}{\partial \mathbf{V}} \\ \dfrac{\partial \mathbf{FQ}_{\text{flow},jk}}{\partial \boldsymbol{\theta}} & \dfrac{\partial \mathbf{FQ}_{\text{flow},jk}}{\partial \mathbf{V}} \end{bmatrix} \begin{bmatrix} \dfrac{\partial \mathbf{P}}{\partial \boldsymbol{\theta}} & \dfrac{\partial \mathbf{P}}{\partial \mathbf{V}} \\ \dfrac{\partial \mathbf{Q}}{\partial \boldsymbol{\theta}} & \dfrac{\partial \mathbf{Q}}{\partial \mathbf{V}} \end{bmatrix}^{-1}_{jk} \tag{3.11}$$

where subscript jk represents contingency jk.

3.3.4 Critical Line Selection

The main objective of this step is to select several transmission lines, called "the critical line", among all transmission lines which have a higher congestion probability with wind integration. To select the critical line, two indicators are implemented.

The first indicator, called the aggregate contingency overload (P_{ACO}), take both the severe contingencies and multiple violations into account as shown in (3.12) [17].

$$P_{ACO,\text{Line}jk}[\%] = \sum_{\substack{\text{Contingencies that} \\ \text{overloaded Line}jk}} (\%\text{Overload} - 100) \tag{3.12}$$

Since overload in the line with higher MVA rating would be more dangerous to the network, it would be more helpful to convert to real MW value as (3.13).

$$P_{ACO,\text{Line}jk} = P_{ACO,\text{Line}jk}[\%] \times MVARating_{\text{Line}jk} \tag{3.13}$$

The second indicator to be considered is with respect to the wind integration. Once wind farm is connected to the grid, it will change the active line

flow through transmission lines. Transmission Line Relief (TLR) sensitivity is utilized to evaluate the impact of wind integration on each line. TLR sensitivity is calculated as shown in (3.14) [18, 19]. It provides the quantitative value of the influence of wind farm on a line.

$$TLR_{\text{Bus } i,\text{Line } jk} = \frac{\Delta MW \text{ Flow}_{\text{Line } lk}}{\Delta MW \text{ Injection}_{\text{Bus } i}} \tag{3.14}$$

3.3.5 Congestion Forecasting

The first task in this step is obtaining the current line flow and variation of scheduled generation and forecasted load. The forecasted line flow of active power can be obtained by (3.15).

$$\begin{bmatrix} \mathbf{P}_{\text{line}}(t) \\ \mathbf{Q}_{\text{line}}(t) \end{bmatrix} = \begin{bmatrix} \mathbf{P}_{\text{line}}(t0) \\ \mathbf{Q}_{\text{line}}(t0) \end{bmatrix} + \alpha \begin{bmatrix} \Delta\mathbf{P}_{\text{inj}} \\ \Delta\mathbf{Q}_{\text{inj}} \end{bmatrix} \tag{3.15}$$

Furthermore, inequality constraint of active power flow in the line can be expressed as (3.16).

$$\alpha\Delta\mathbf{P}_{\text{inj}} \leq (\mathbf{P}_{\text{limit}} - \mathbf{P}_{\text{original}}) \tag{3.16}$$

where $\mathbf{P}_{\text{limit}}$ is a vector of active power line flow limit and $\mathbf{P}_{\text{original}}$ is a vector of original active power line flow.

3.3.6 Evaluation of Other Scenario

If any constraint violates, other scenarios need to be evaluated to avoid congestion, such as re-dispatch of a generation or the lower wind penetration level. For evaluating other scenarios, (3.15) should be also utilized, but active power injection would be different from original scenarios.

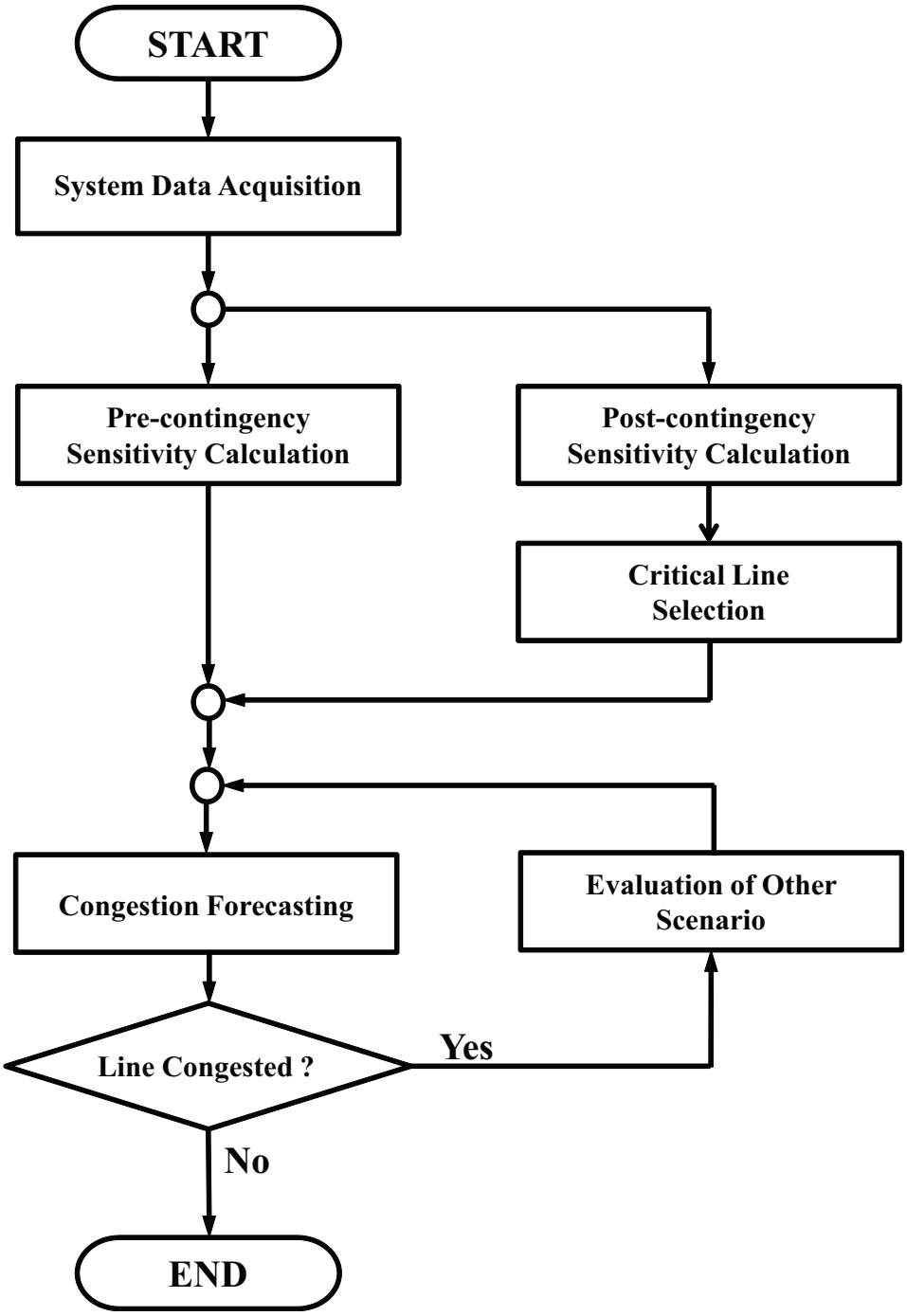

Figure 3.1: Flowchart of Congestion Forecasting Procedure

Chapter 4

Pilot Bus Selection

4.1 Introduction

In this chapter, a novel technique for pilot bus selection among all load buses is introduced to provide information about power system instability. The integration of large wind wind farms may cause instability of the network because wind has an intermittent characteristic. Also since wind turbine may absorb reactive power of the system, voltage throughout system may require more reactive power support [22]. Selecting a pilot bus and predicting the voltage level at the bus are advantageous with respect to preventing voltage collapse of the entire system. This technique is performed based on sensitivity analysis and loading margin calculated by continuation power flow. Furthermore, by predicting the voltage profile at the pilot bus, it is possible to know when the voltage of the entire network can collapse and to prepare reactive power support.

4.2 Loading Margin

The most common method to analyze the voltage stability of a network is bifurcation theory. The theory is built to express system instability with

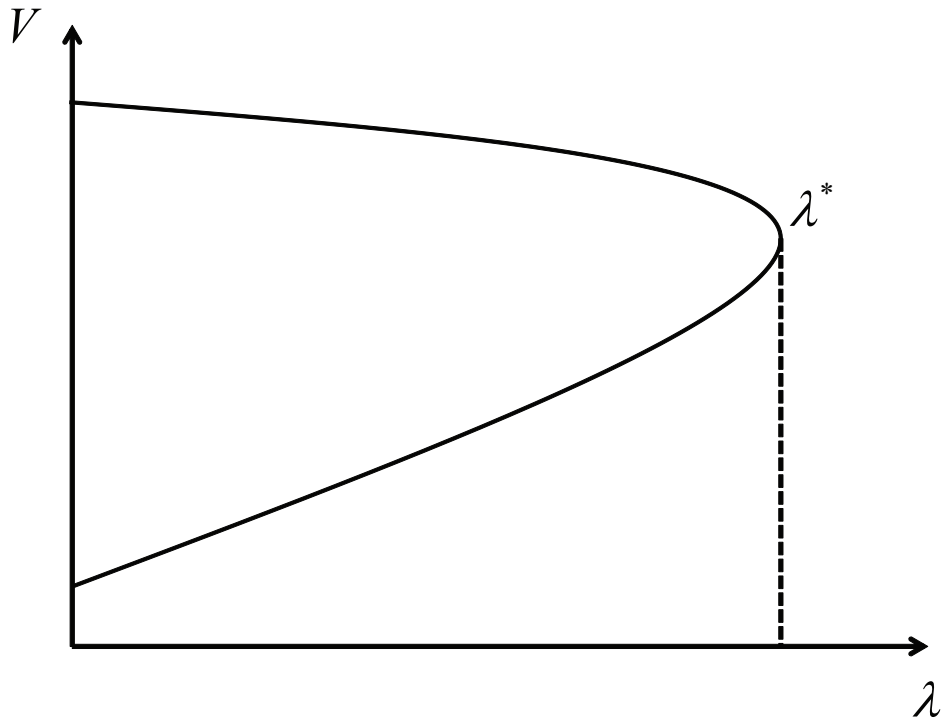

Figure 4.1: PV Curve

quantitative values on how far the system is from the voltage collapse point. This index is very helpful in providing important information of voltage stability to system operators [32]. According to the theory, the system equation can be expressed with one parameter, so called "loading parameter (λ)" as follows in (4.1).

$$0 = f(x, \lambda) \tag{4.1}$$

where x is system variables such as voltage magnitude and angle.

In (4.1), loading parameter λ as the slowly changing load parameter

that specifies the changes in the active power injection of load and generation as (4.2) and (4.3) and finally it can find the collapse point of loading parameter λ^* [10, 25].

$$P_G = (1+\lambda)(P_{G_0} + P_S) \tag{4.2}$$

$$P_L = (1+\lambda)(P_{L_0} + P_D) \tag{4.3}$$

where P_{G0} is active power injection of generation and P_{L0} is active power injection of load at the basecase.

Figure 4.1 shows the relationship between the loading parameter and voltage, which is so called "nose curve". In the figure, λ^* express voltage collapse point, so that at that point, if loading parameter increases more, voltage will collapse and the system may fall under serious condition with loss of the load.

4.3 Continuation Power Flow

Continuation power flow is widely utilized to find nose curve shown in Figure 4.1 from the power flow equations with loading parameter λ. The method is valuable to pinpoint bifurcation, which is critical point with respect to voltage stability. Furthermore, it determines the proximity to voltage collapse. It uses a predictor-corrector scheme to find a solution path of a set of power flow formulations as shown in Figure 4.2 [5, 28].

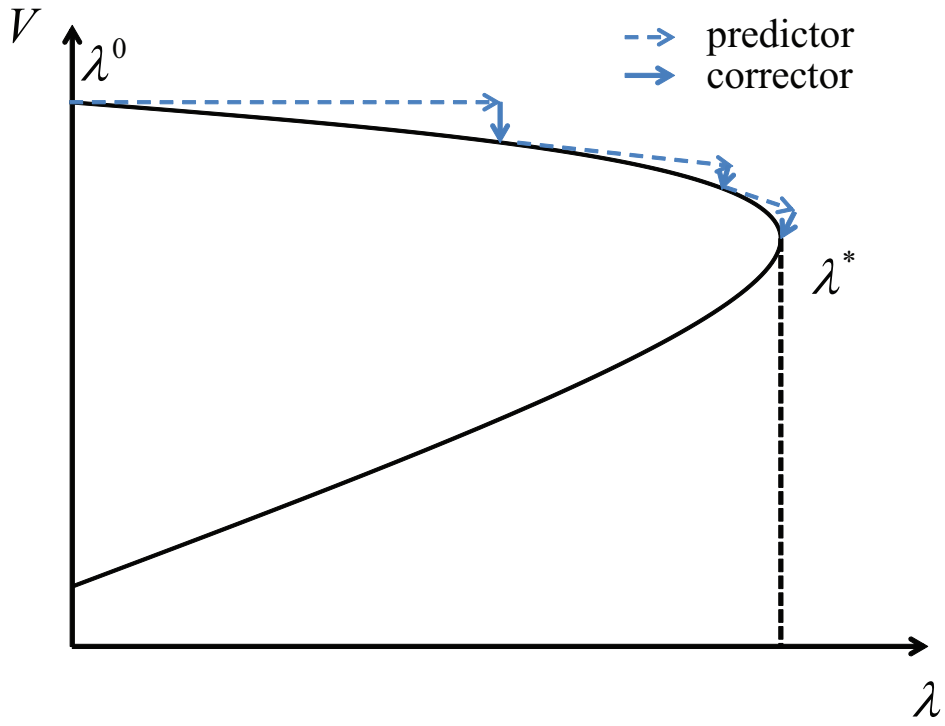

Figure 4.2: An illustration of the predictor-corrector method

4.4 Pilot Bus Selection Procedure

The flowchart for pilot bus selection is shown in Figure 4.3. And the description of each part follows below.

4.4.1 System data acquisition

At this step, the information about the system is obtained, such as generator, load and transmission line.

- Generator information : P_{Gmax}, P_{Gmin}, Q_{Gmax}, and Q_{Gmin}
- Load information : P_L and Q_L
- Transmission Line information : $R_{jk} + iG_{jk}$ and $P_{jk,\mathrm{lim}}$

4.4.2 Contingency screening

Since size of real system is excessively large, the contingency screening process is needed to prevent lengthy process. This screening is performed based on loading margin when contingency occurs. When line outage occurs, maximum load parameter is reduced, which means that the system becomes closer to voltage collapse point. It can be said that the contingency which has less value of maximum loading parameter is more critical [11].

4.4.3 Contingency analysis for observability

As one of the criteria to select pilot bus, observability should be taken into account. In other words, voltage at the pilot bus should be representative of voltage values of all buses. In order to satisfy the criterion loading margin

and voltage deviation can be utilized based on N-1 contingency. The first objective function can be expressed as (4.4).

$$J_1^i = \sum_{jk \in \Omega_C} \lambda_{jk} \times \frac{1}{|\Delta V_{i,jk}|} \tag{4.4}$$

where Ω_C represents every contingency, λ_{jk} is maximum value of loading parameter at contingency jk, and $\Delta V_{i,jk}$ is the voltage deviation at bus i after contingency jk.

4.4.4 Sensitivity analysis for controllability

The second criterion is controllability, which utilizes centralized control scheme. In other words, reactive power from every generator controls the voltage at the pilot bus. Therefore, sensitivity of $\frac{\partial V_{\text{pilot}}}{\partial Q_{\text{G}}}$ should be taken into account.

Generally, for the Newton-Raphson method, Jacobian matrix is formulated as shown in (4.5) [7].

$$\mathbf{J} = \begin{bmatrix} \mathbf{J_{P\theta}} & \mathbf{J_{PV}} \\ \mathbf{J_{Q\theta}} & \mathbf{J_{QV}} \end{bmatrix} = \begin{bmatrix} \frac{\partial \mathbf{P}}{\partial \boldsymbol{\theta}} & \frac{\partial \mathbf{P}}{\partial \mathbf{V}} \\ \frac{\partial \mathbf{Q}}{\partial \boldsymbol{\theta}} & \frac{\partial \mathbf{Q}}{\partial \mathbf{V}} \end{bmatrix} \tag{4.5}$$

It should be noted that $\mathbf{J}$ refers Jacobian matrix in (4.5). The $\mathbf{J_{QV}}$ part of the Jacobian matrix represents sensitivity of reactive power to voltage. The pilot bus sensitivity can be obtained from $\mathbf{J_{QV}}$.

The second part of objective function is represented as (4.6).

$$J_2^i = -\sum_{l \in \Omega_G} \frac{\Delta V_i}{\Delta Q_l} \tag{4.6}$$

where Ω_G refers to every generator.

4.4.5 Objective Function Evaluation

Finally objective function to choose the pilot bus can be expressed as (4.7).

$$J_i^\star = \min_{i \in \Omega_D} J^i = \min_{i \in \Omega_D} \alpha_1 J_1^i + \alpha_2 J_2^i \tag{4.7}$$

where α_1 and α_2 are normalized weights.

The bus which has the minimum value of the objective function ($J_i^\star$) is chosen as the pilot bus, which satisfies two important criteria, that it is representative among all buses and that it is readily controllable by reactive power generation. Furthermore, forecasting the voltage at the pilot bus is highly useful for a system operator to know when the voltage collapse would occur and to readily regulate the voltage stability by reactive power support.

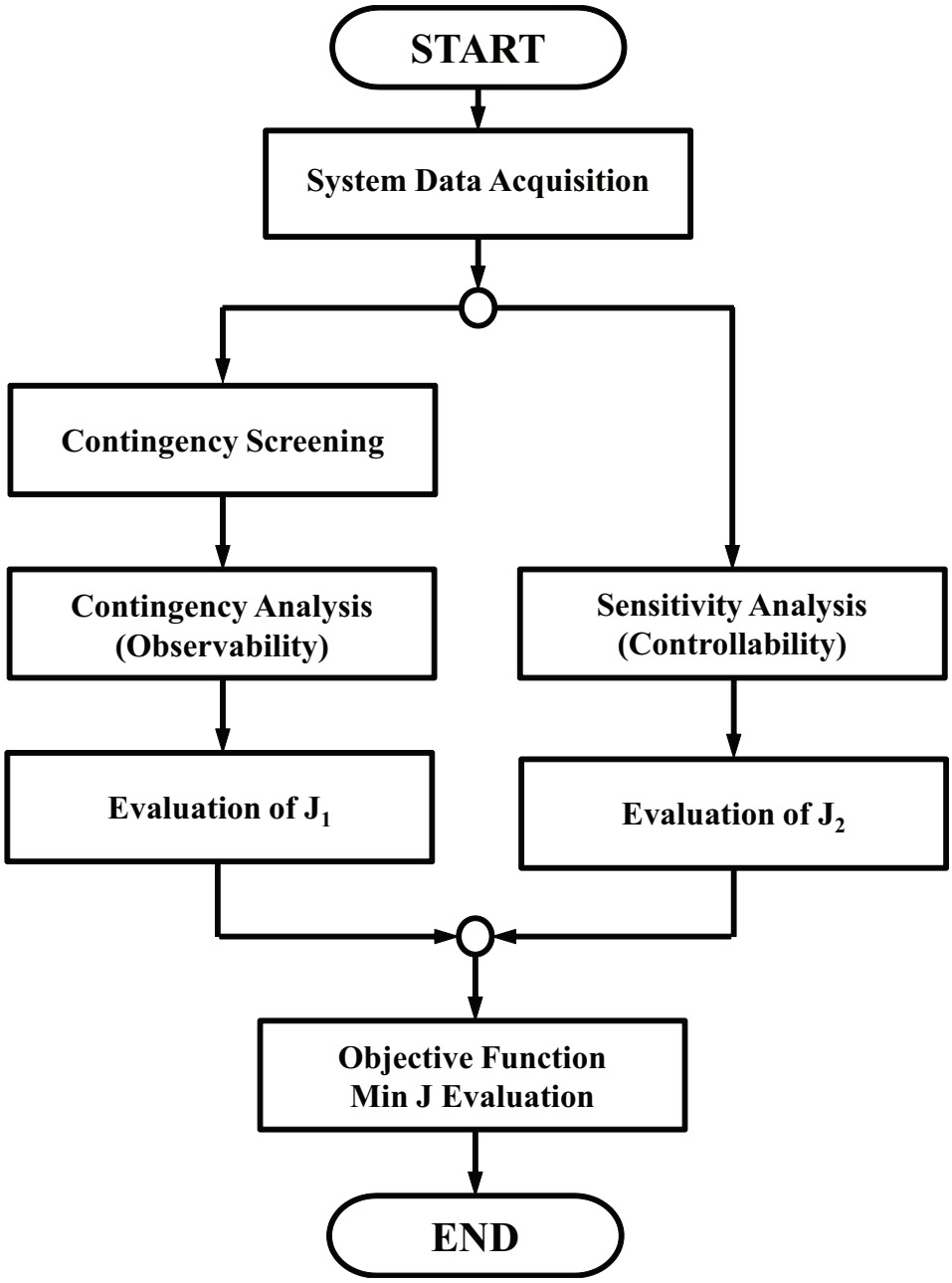

Figure 4.3: Flowchart of pilot bus selection

Chapter 5

Case Studies and Discussion

5.1 Introduction

This chapter describes simulation results from two case studies for forecasting transmission line congestion, pilot bus selection, and predicting the voltage profile at the pilot bus of a system with wind power generation. For the simulation, MATLAB-based Power System Analysis Tool (PSAT) [27] and Powerworld simulator are used.

5.2 IEEE 14-Bus test system

IEEE 14-bus test system, which represents a portion of the American Electric Power system (in the Midwestern US), is simulated for the first case study. The test system includes two generators and three synchronous condensers located at buses 1, 2, 3, 6, and 8, respectively. It also consists of twenty branches and fourteen buses with eleven loads having total demand of 259 MW and 81.4 MVar at the base case.

In order to evaluate impact of wind integration, one more bus is added and one wind farm (P_{wind} = 100MW) is connected to the bus as shown in

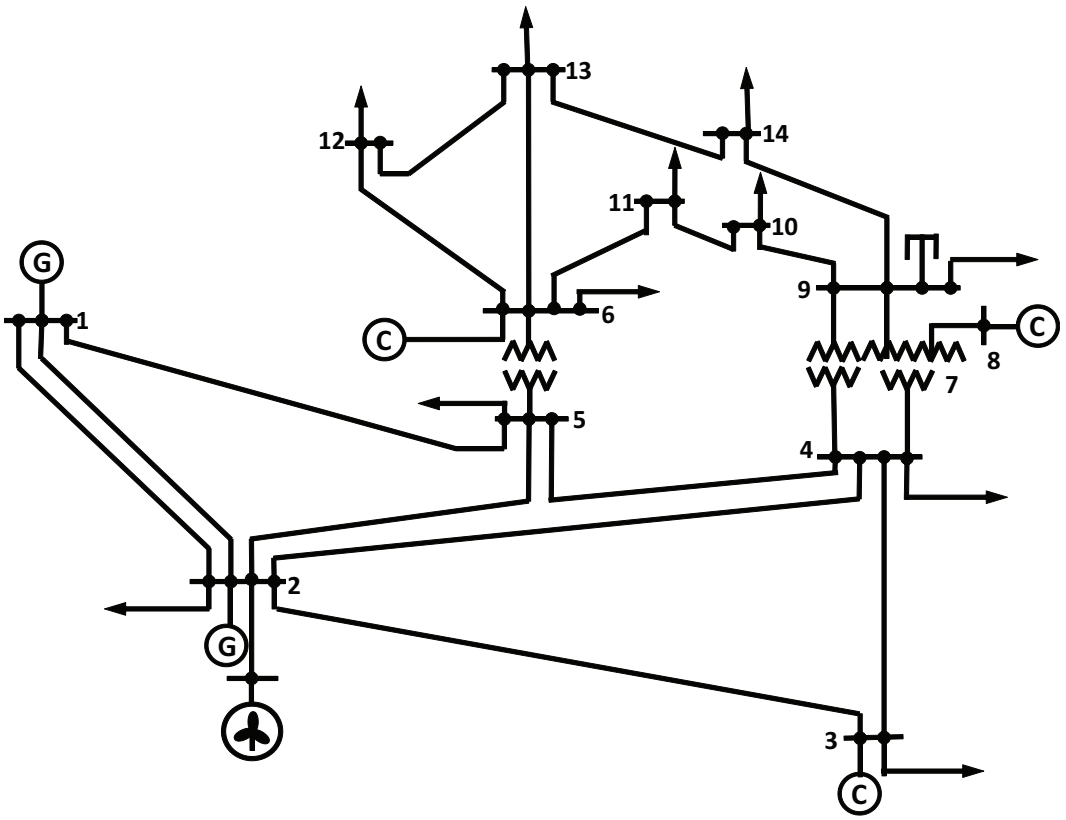

Figure 5.1: IEEE 14-bus system with wind farm

Figure 5.1.

5.2.1 Pilot Bus Selection

The first step of the simulation is contingency screening to reduce calculations. For contingency screening, the result of the maximum loading parameter evaluation after each contingency is shown in Table 5.1 for the contingencies that have the greatest effect on on voltage stability.

Con jk	**Basecase**	1 TO 2	2 TO 3	5 TO 6	7 TO 9	6 TO 13
$\lambda_{\max}$	**4.0678**	1.7275	2.2675	2.2811	2.8659	3.2255
$\Delta\lambda_{\max}$	0	2.3403	1.8003	1.7867	1.2019	0.8423

Table 5.1: Maximum Loading Parameter after Contingency jk

According to the result, five contingencies (1 TO 2, 2 TO 3, 5 TO 6, 7 TO 9, 6 TO 13) would be taken into account to select pilot bus, because the contingencies have more significant influence on the system with respect to the voltage stability than the other contingencies.

Figure 5.2 shows the change of the nose curve of the system after the

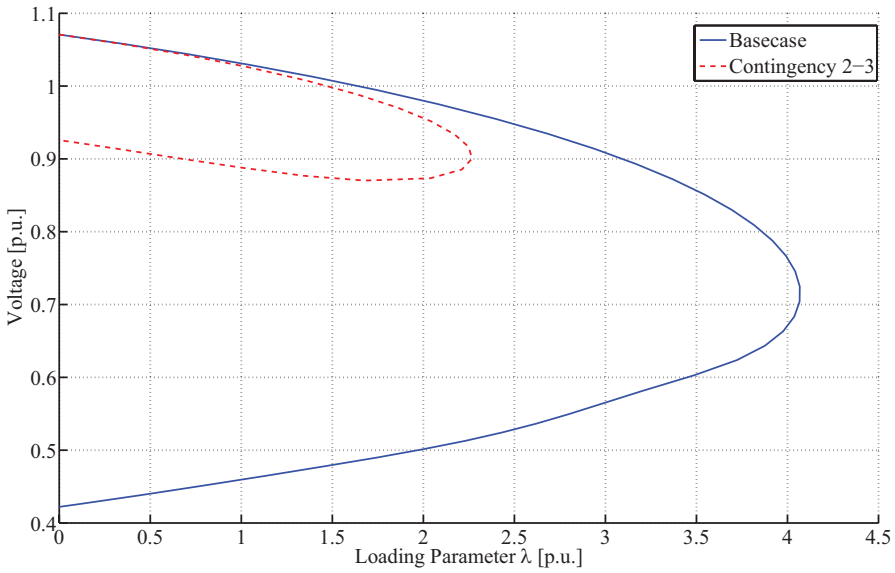

Figure 5.2: Nose curve at basecase and contingency (2-3)

contingency (2 TO 3). As shown in the figure, the maximum loading parameter decreases significantly after the contingency. It can also be said that the

loadability and voltage stability of the system decrease after the contingency occurs.

In order to select the pilot bus, the objective function is evaluated. As

	Bus 4	Bus 5	Bus 7	Bus 9	Bus 10	**Bus 11**	Bus 12	Bus 13
$\boldsymbol{J_i}$	254.10	59.93	28.67	11.31	13.87	**11.17**	188.41	73.44

Table 5.2: Result of objective function for pilot bus selection

shown in Table 5.2, bus #11 is chosen as the pilot bus because bus #11 has the minimum value of the objective function.

Figure 5.3 shows the dependence of bus voltage on pilot bus voltage

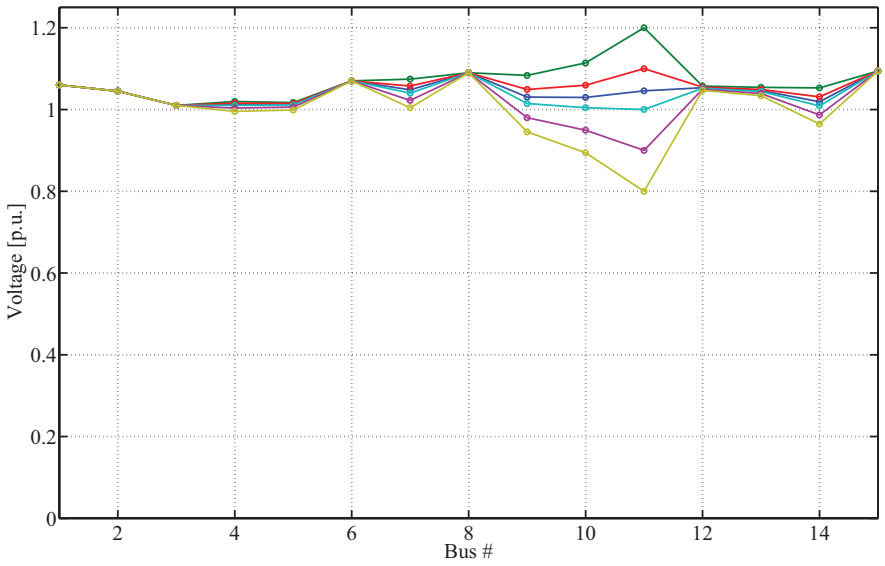

Figure 5.3: Voltage profile change with varying choices of pilot bus voltage

with varying choices of pilot bus. As varying voltage level (0.8 p.u. – 1.2 p.u.) at the pilot bus, voltage level at other buses also change. Accordingly, it can

be said that the pilot bus is representative and the voltage level throughout the network can be controlled by the pilot bus voltage level.

5.2.2 Congestion Forecasting

Contingency	1 TO 5	1 TO 2	2 TO 4	3 TO 4	4 TO 5
L_0000011-0000022C1	46.47	-	-	-	-
L_0000011-0000055C1	-	43.79	-	-	-
L_0000022-0000033C1	-	-	0.32	1.12	2.3
L_0000022-0000044C1	-	57.93	-	-	-
Total [MW]	46.47	101.72	0.32	1.12	2.3

Table 5.3: PACO result of 14-bus system

First task for congestion forecasting is to rank the transmission lines and to select the critical lines using two indicators. The first indicator to rank the lines is the aggregate contingency overload (P_{ACO}) as shown in (3.12). Table 5.3 shows the result of P_{ACO} evaluation of the test system. This indicator provides the information on the summation of overloaded active line flow after every contingency.

The second indicator in selecting critical line is the TLR sensitivity

	1 TO 5	1 TO 2	3 TO 4	4 TO 5	2 TO 4
|TLR| (Bus 15)	0.2198	0.1533	0.0517	0.0532	0.0161

Table 5.4: TLR sensitivity result on 14-bus system

as calculated by (3.14). Through the result of the indicator, the quantitative relation between active line flow in lines and connected wind power can be

obtained. The calculated result is shown in Table 5.4. The absolute value of TLR sensitivity is the objective of evaluation because amount of the impact is the variable of interest.

According to the two indicators, five lines (1 TO 5, 1 TO 2, 3 TO 4, 4 TO 5, 2 TO 4) are chosen as the critical lines and will be forecasted. It can be said that the five lines are more critical of being congested after contingencies and are impacted more by the installed wind farm.

In order to simulate the scenario, the load and wind profile for the

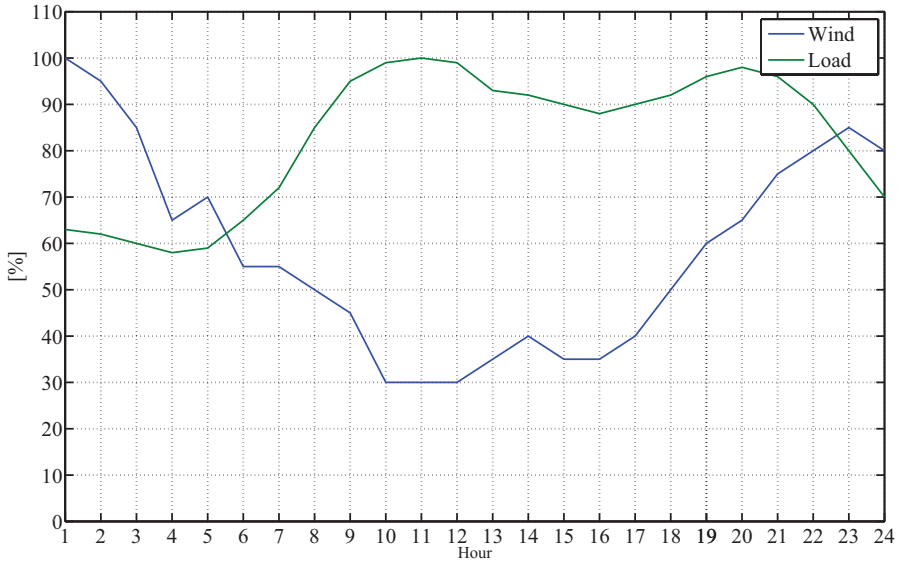

Figure 5.4: Load and Wind profile for 24 hours

next 24 hours are assumed as shown in Figure 5.4. Generally, load consumption peaks at the daytime and wind power peaks at the nighttime for Texas onshore wind as shown in the figure. Other thermal generators are dispatched

according to the ratio of generation at base case. This is only a rough approximation to actual dispatch,

Through the proposed approach to forecast congestion, the pre-contingency

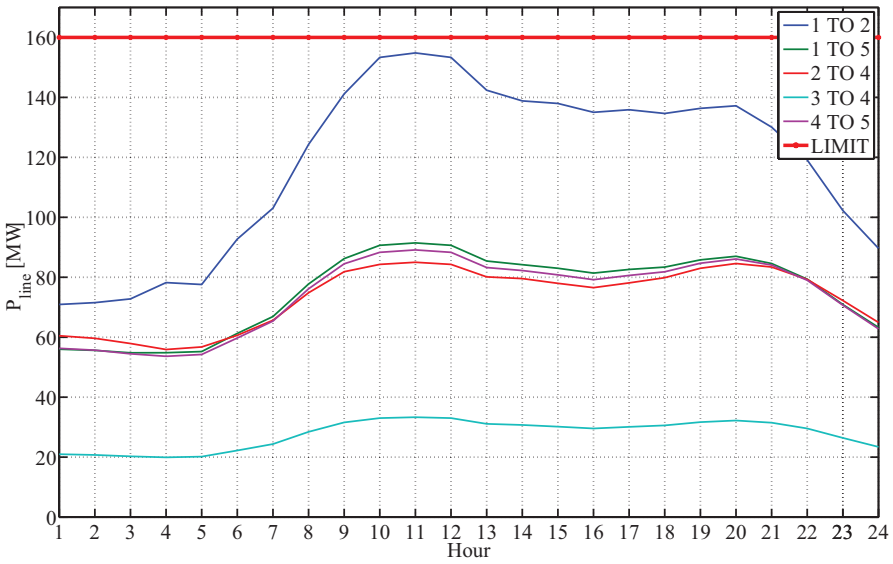

Figure 5.5: Active Line Flow for 24 hours

sensitivity matrix α can be obtained. The active line flow for 24 hours is forecasted as shown in Figure 5.5. According to the result, none of the lines are congested at any given time at the pre-contingency condition.

By the previous pilot bus selection and reactive power sensitivity analysis, the voltage profile at the pilot bus can also be predicted by (5.1) as shown in Figure 5.6,

$$V_{\text{Pilot}}(t) = V(t0) + \sum_{j \in \Omega_G} \frac{\Delta V}{\Delta Q_j} \Delta Q_j \tag{5.1}$$

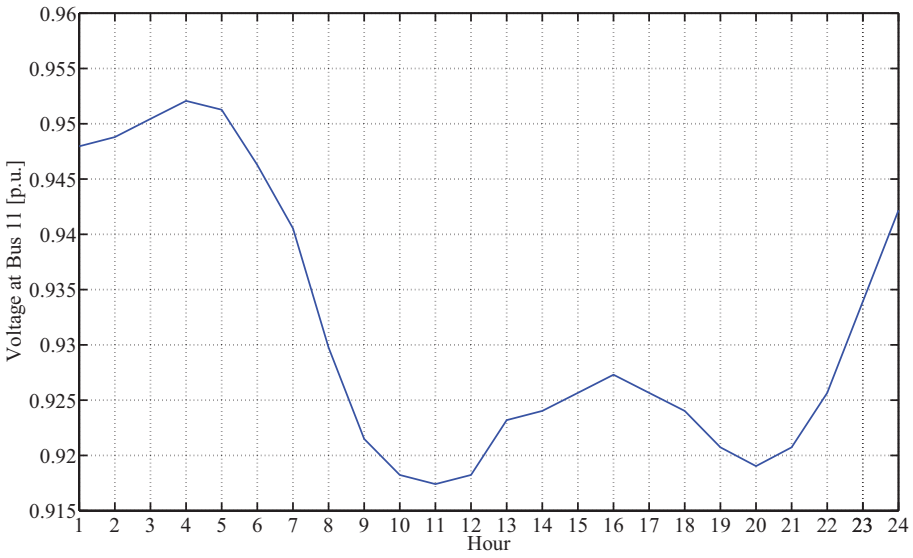

Figure 5.6: Voltage Profile at the Pilot Bus (Bus #11) for 24 hours

where Ω_G represents every generator. This relation represents the voltage profile at the pilot bus (bus #11) as well as the voltage stability of the entire system because the pilot bus is representative of the voltage profile of the entire system.

By predicting the voltage profile at the pilot bus, the timing of reactive power support needs can be determined. It would be highly beneficial to reliably operate the system.

Also, Figure 5.7 shows the forecasted reactive power flow according to the scheduled load demand. The reactive power flow also can be predicted in the same way as the active line flow forecasting; however, reactive power flows

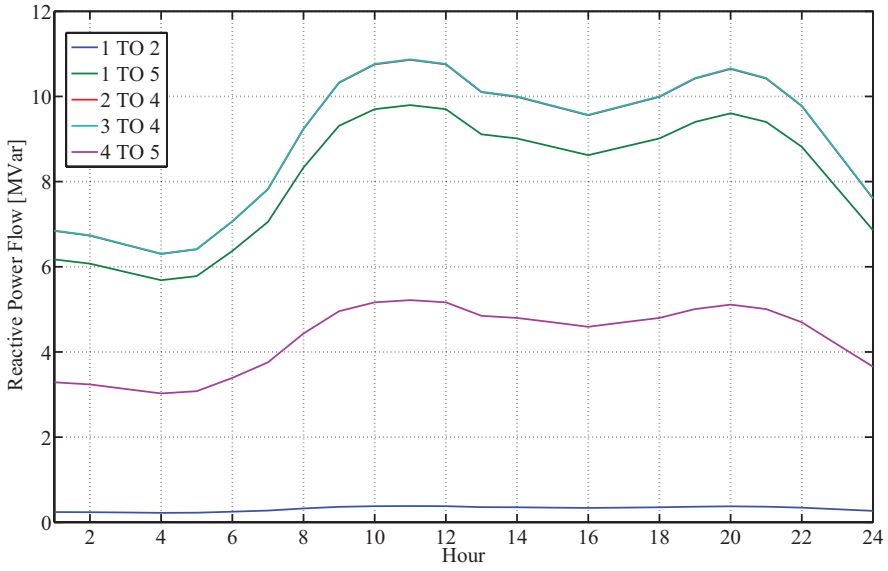

Figure 5.7: Reactive Line Flow for 24 hours

will generally be less accurately presented than real power flows.

5.3 IEEE 39-Bus Test System

The single line diagram of the IEEE 39-bus test system is shown in Figure 5.8 for the second case study. The test system includes 10 generators located at buses 30, 31, 32, 33, 34, 35, 36, 37, 38, and 39, respectively. It also consists of 46 transmission lines and 39 buses with 19 loads having total demand of 6097.1 MW and 1408.9 MVar at the base case. In order to simulate the situation of wind integration, two more buses are added and two wind farms ($P_{\text{wind}} = 100MW$) are connected to the buses.

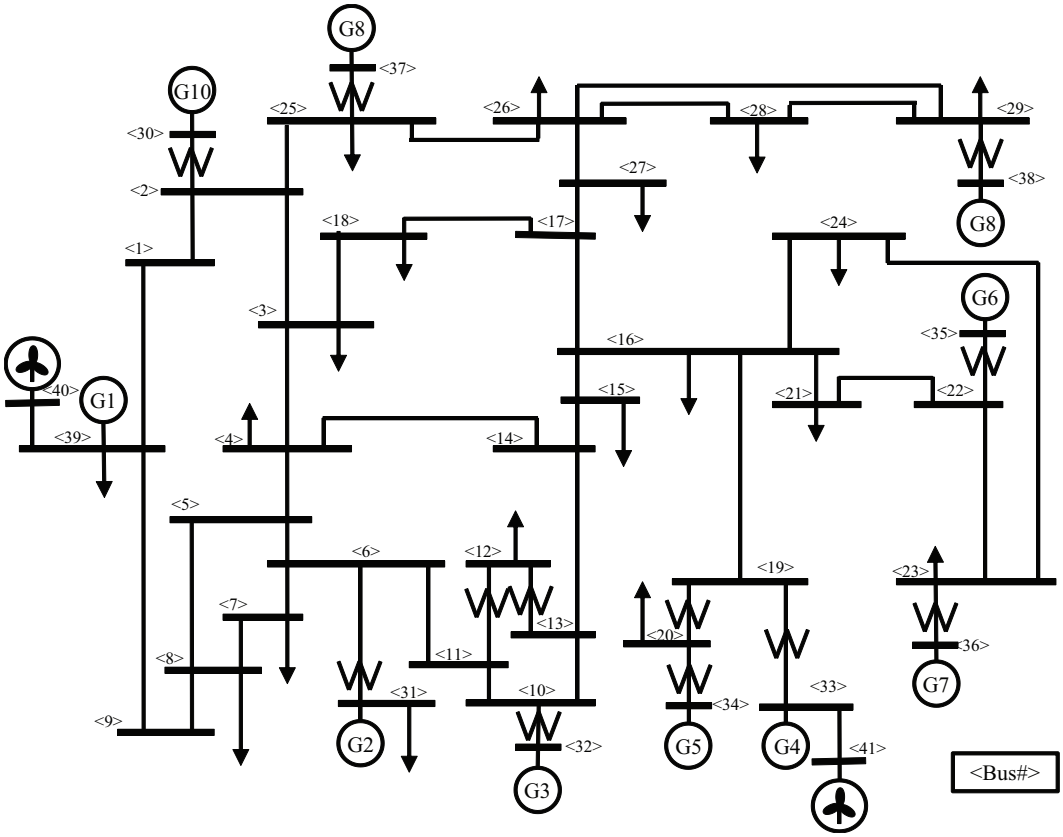

Figure 5.8: IEEE 39-bus system with wind farm

5.3.1 Pilot Bus Selection

As in the previous case study, to avoid a lengthy process, only five contingencies are selected based on maximum loading parameter evaluation as shown in Table 5.5. It can be said that the five contingencies makes more significant influence with respect to voltage stability.

Also, the result of evaluation of the objective function is shown in Table 5.6. Bus # 16 has the minimum value of the objective function according to the result. Therefore, the bus # 16 is selected as the pilot bus to be forecasted.

Con jk	Basecase	21 TO 22	15 TO 16	28 TO 29	2 TO 3	16 TO 21
$\lambda_{\max}$	2.2274	1.5537	1.6335	1.7396	1.9462	1.9723
$\Delta\lambda_{\max}$	0	0.6737	0.5939	0.4878	0.2812	0.2551

Table 5.5: Maximum Loading Parameter after Contingency jk

	Bus 3	Bus 15	**Bus 16**	Bus 18	Bus 24
$\boldsymbol{J^i}$	4.984922	4.265626	**3.541753**	4.360164	3.967153

Table 5.6: Result of objective function for pilot bus selection

5.3.2 Congestion Forecasting

	16 TO 17	17 TO 27	3 TO 18	23 TO 24
P_{ACO} [MW]	778.2	660.6	650.26	615.98

Table 5.7: P_{ACO} result of 39-bus system

Table 5.7 shows the P_{ACO} result for the 39-bus system. In the system there are 48 transmission lines, selecting critical lines and forecasting the lines would be an efficient way to avoid excessive calculation. The result of P_{ACO} provides the most effective evaluation to select the critical lines among all the lines. According to the result, four lines are chosen as the critical lines, which means that these four lines are of greatest concern when a contingency occurs.

The second indicator is the TLR sensitivity, which provides the quantitative value of the impact of wind power on each line. The results are shown in Table 5.8. Based on the result, five more lines are selected for the critical lines.

For the simulation, the load and wind profile for the next 24 hours is

	16 TO 19	19 TO 33	16 TO 17	1 TO 2	1 TO 39
TLR1 (Bus #40)	0.2526	0.1778	-0.2139	0.4174	-0.4174
TLR2 (Bus #41)	-0.7474	-0.8222	0.3697	-0.0893	0.0893
|TLR1| + |TLR2|	1.0000	1.0000	0.5836	0.5067	0.5067

Table 5.8: TLR result of 39-bus system

assumed to be the same as the previous case study as shown in Figure 5.4.

Finally, Figure 5.9 shows the result of the forecast of active line flow

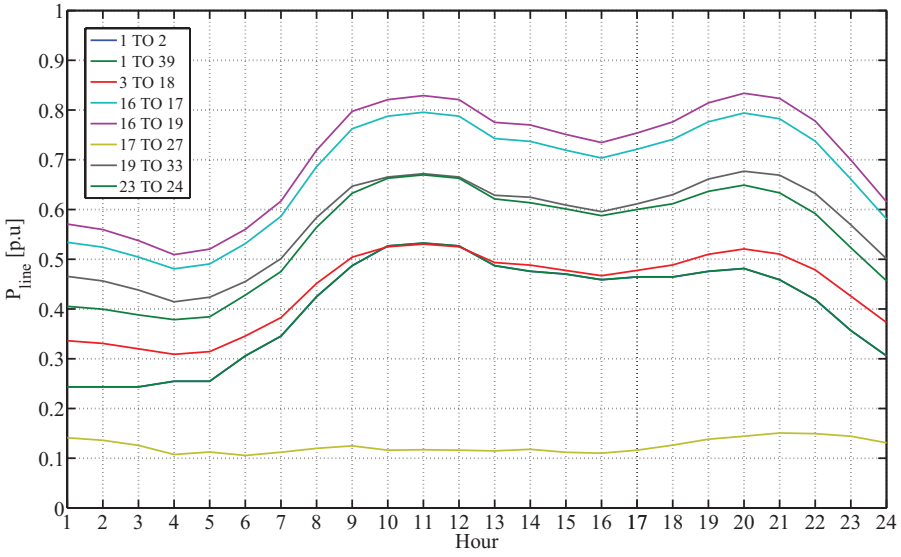

Figure 5.9: Active Power Flow at Pre-Contingency

based on pre-contingency analysis. In the figure, the values of active power flow are normalized by the thermal limit of each line. In this case, none of constraints of active line flow are violated.

The prediction of voltage profile at the pilot bus (bus #16) is shown in Figure 5.10.

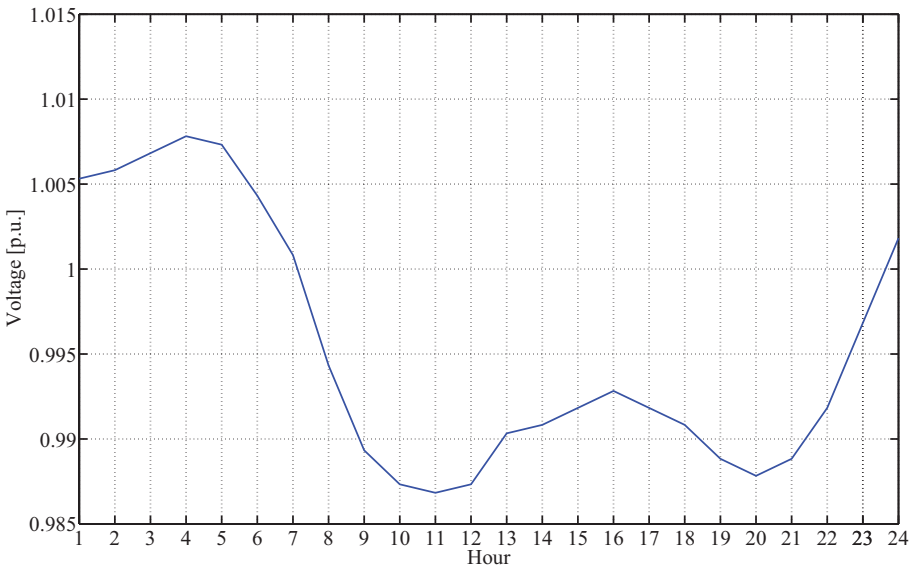

Figure 5.10: Voltage Profile at the Pilot Bus (Bus #16)

In order to simulate post-contingency, the same procedure is performed with post-contingency (22 TO 23) sensitivity matrix β_{jk}. As a result shown in Figure 5.11, the line (23 TO 24) is violated. In this case, the system operator should take a remedial action to avoid the congestion

Also, the reactive power flow through the critical lines can be predicted as shown in Figure 5.12.

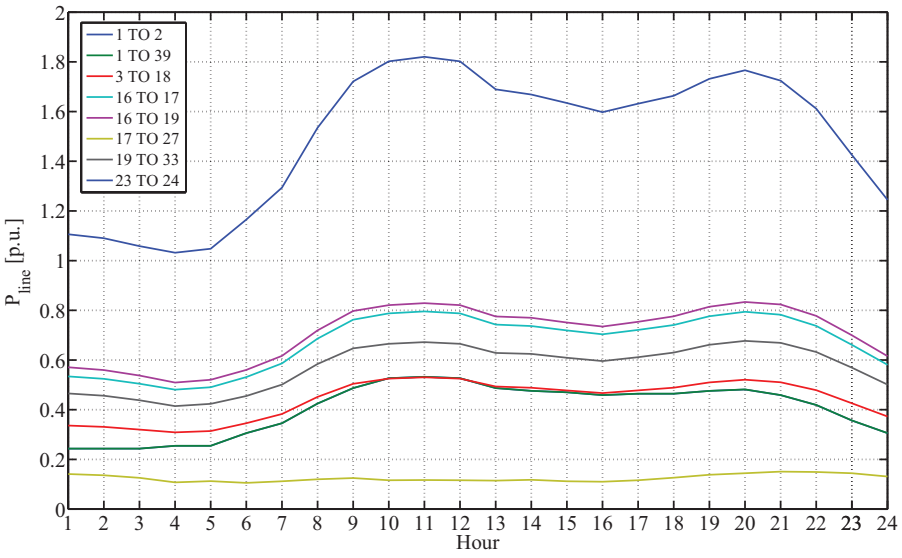

Figure 5.11: Active Power Flow at Post-Contingency (22 TO 23)

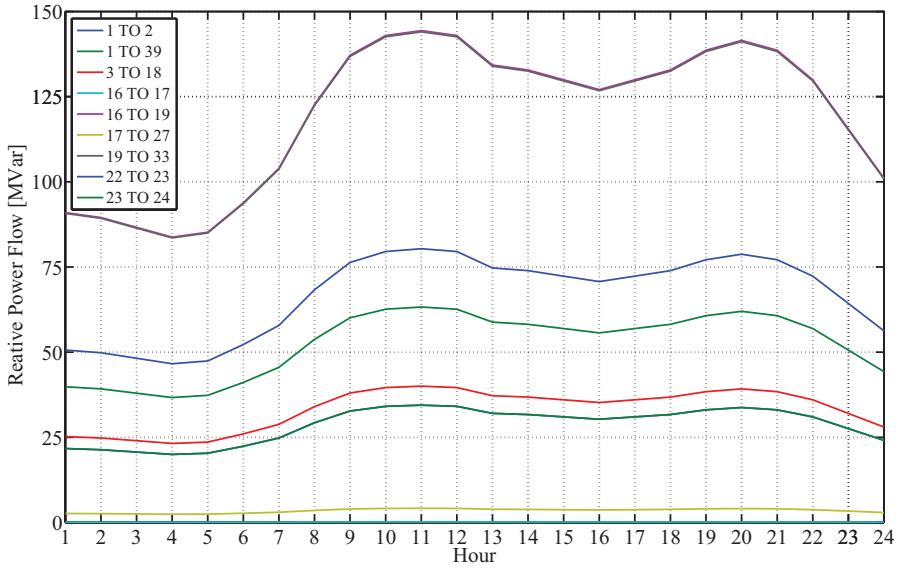

Figure 5.12: Reactive Power Flow at Pre-Contingency

Chapter 6

Conclusion and Future Work

6.1 Conclusion

In this thesis, a technique to forecast congestion in transmission lines in systems with wind power integration based on sensitivity analysis is proposed. Additionally, a problem is solved to select a pilot bus in the network to predict voltage stability. The following can be concluded:

1. A technique to forecast the congestion based on sensitivity analysis was performed. P_{ACO} and TLR sensitivity are useful indicators to determine which line is more critical. By calculating pre-contingency sensitivity matrix α and post-contingency sensitivity matrix β_{jk}, transmission line congestion before and after a contingency can be forecasted.

2. With this technique, it is possible for system operators to know when and where the congestion occurs. It is highly useful to support decisions and to prepare a remedial action to avoid the congestion.

3. Additionally, the pilot bus selection is performed to find the bus that is representative and readily controllable. Based on continuation power flow, N-1 contingency, and sensitivity analysis, a pilot bus is selected

among all load buses. Taking the important factors into consideration, the pilot bus can be chosen with two significant criteria, observability and controllability.

4. By predicting the voltage profile at the pilot bus, the information of voltage stability can be given to system operators. Furthermore it would be very beneficial to prepare reactive power support.

5. Finally, two case studies with test systems were simulated successfully. Active line flow as well as voltage profile at the pilot bus could be forecasted for next 24 hours.

6.2 Future Work

This thesis provides a variety of topics for future investigations as follows:

1. This forecasting technique can include probabilistic study for wind power and load to estimate probability of congestion and voltage instability.

2. A control method can be developed to avoid transmission line congestion such as re-dispatch or wind power reduction.

3. A control technique to enhance stability such as installation of FACTS (Flexible Alternating Current Transmission System) device such as SVC (Static VAr Compensator) and reactive power control of generators can be developed.

4. With cost model of generation and load, more accurate dispatch of generation and consumption can be investigated.

Appendices

Appendix A

Test System Data

A.1 IEEE 14-bus Test System

```
Bus.con = [ ...
1 69 1 0 4 1;
2 69 1 0 4 1;
3 69 1 0 4 1;
4 69 1 0 4 1;
5 69 1 0 4 1;
6 13.8 1 0 2 1;
7 13.8 1 0 2 1;
8 18 1 0 3 1;
9 13.8 1 0 2 1;
10 13.8 1 0 2 1;
11 13.8 1 0 2 1;
12 13.8 1 0 2 1;
13 13.8 1 0 2 1;
14 13.8 1 0 2 1;
15 69 1 0 1 1;
];


Line.con = [ ...
2 5 100 69.0 60 0 0.000000 0.05695 0.17388 0.0340 0.000 0 0 0 0 1;
6 12 100 13.8 60 0 0.000000 0.12291 0.25581 0.0000 0.000 0 0 0 0 1;
12 13 100 13.8 60 0 0.000000 0.22092 0.19988 0.0000 0.000 0 0 0 0
1;
6 13 100 13.8 60 0 0.000000 0.06615 0.13027 0.0000 0.000 0 0 0 0 1;
6 11 100 13.8 60 0 0.000000 0.09498 0.1989 0.0000 0.000 0 0 0 0 1;
```

```
11 10 100 13.8 60 0 0.000000 0.08205 0.19207 0.0000 0.000 0 0 0 0
1;
9 10 100 13.8 60 0 0.000000 0.03181 0.0845 0.0000 0.000 0 0 0 0 1;
9 14 100 13.8 60 0 0.000000 0.12711 0.27038 0.0000 0.000 0 0 0 0 1;
14 13 100 13.8 60 0 0.000000 0.17093 0.34802 0.0000 0.000 0 0 0 0
1;
7 9 100 13.8 60 0 0.000000 0.00000 0.11001 0.0000 0.000 0 0 0 0 1;
1 2 100 69.0 60 0 0.000000 0.01938 0.05917 0.0528 0.000 0 0 0 0 0;
15 2 100 69.0 60 0 0.000000 0.10000 0.40000 0.1000 0.000 0 0 0 0 1;
3 2 100 69.0 60 0 0.000000 0.04699 0.19797 0.0438 0.000 0 0 0 0 1;
3 4 100 69.0 60 0 0.000000 0.06701 0.17103 0.0346 0.000 0 0 0 0 1;
1 5 100 69.0 60 0 0.000000 0.05403 0.22304 0.0492 0.000 0 0 0 0 1;
5 4 100 69.0 60 0 0.000000 0.01335 0.04211 0.0128 0.000 0 0 0 0 1;
2 4 100 69.0 60 0 0.000000 0.05811 0.17632 0.0374 0.000 0 0 0 0 1;
4 9 100 69.0 60 0 5.000000 0.00500 0.55618 0.0000 0.969 5 0 0 0 1;
5 6 100 69.0 60 0 5.000000 0.00000 0.25202 0.0000 0.932 0 0 0 0 1;
4 7 100 69.0 60 0 5.000000 0.00000 0.20912 0.0000 0.978 0 0 0 0 1;
8 7 100 18.0 60 0 1.304348 0.00000 0.17615 0.0000 0.000 0 0 0 0 1;
];


SW.con = [ ...
1 100 69 1.06 0 9.9 -9.9 1.2 0.8 2.324 1 1 1;
];


PV.con = [ ...
2 100 69.0 0.4 1.045 0.50 -0.40 1.2 0.8 1 1;
6 100 13.8 0.0 1.070 0.24 -0.06 1.2 0.8 1 1;
3 100 69.0 0.0 1.010 0.40 0.00 1.2 0.8 1 1;
8 100 18.0 0.0 1.090 0.24 -0.06 1.2 0.8 1 1;
];


PQ.con = [ ...
11 100 13.8 0.035 0.018 1.2 0.8 0 1;
```

```
13 100 13.8 0.135 0.058 1.2 0.8 0 1;
3 100 69.0 0.942 0.190 1.2 0.8 0 1;
5 100 69.0 0.076 0.010 1.2 0.8 0 1;
2 100 69.0 0.217 0.127 1.2 0.8 0 1;
6 100 13.8 0.112 0.075 1.2 0.8 0 1;
4 100 69.0 0.478 -0.040 1.2 0.8 0 1;
14 100 13.8 0.149 0.050 1.2 0.8 0 1;
12 100 13.8 0.061 0.016 1.2 0.8 0 1;
10 100 13.8 0.090 0.058 1.2 0.8 0 1;
9 100 13.8 0.295 0.166 1.2 0.8 0 1;
];


PQgen.con = [ ...
15 100 69 1 0 1.1 0.9 0 1;
];


Bus.names = ...
'Bus 01'; 'Bus 02'; 'Bus 03'; 'Bus 04'; 'Bus 05';
'Bus 06'; 'Bus 07'; 'Bus 08'; 'Bus 09'; 'Bus 10';
'Bus 11'; 'Bus 12'; 'Bus 13'; 'Bus 14'; 'Bus1';
```

A.2 IEEE 39-bus Test System

```
Bus.con = [ ...
1 154.00 1.03627 -0.07968 1 1;
2 154.00 1.01900 -0.03718 1 1;
3 154.00 0.99068 -0.09283 1 1;
4 154.00 0.95515 -0.12134 1 1;
5 154.00 0.95492 -0.10930 1 1;
6 154.00 0.95617 -0.09849 1 1;
7 154.00 0.94821 -0.13751 1 1;
```

```
8 154.00 0.94886 -0.14549 1 1;
9 154.00 1.00876 -0.12110 1 1;
10 154.00 0.96231 -0.04422 1 1;
11 154.00 0.95881 -0.06261 1 1;
12 154.00 0.93924 -0.06024 1 1;
13 154.00 0.96056 -0.05583 1 1;
14 154.00 0.96088 -0.08230 1 1;
15 154.00 0.96781 -0.07346 1 1;
16 154.00 0.98685 -0.03947 1 1;
17 154.00 0.99123 -0.06315 1 1;
18 154.00 0.98951 -0.08259 1 1;
19 154.00 0.98850 0.07679 1 1;
20 154.00 0.98630 0.05952 1 1;
21 154.00 0.99417 0.00551 1 1;
22 154.00 1.02099 0.08776 1 1;
23 154.00 1.01966 0.08379 1 1;
24 154.00 0.99525 -0.03729 1 1;
25 154.00 1.02804 -0.01112 1 1;
26 154.00 1.01715 -0.03141 1 1;
27 154.00 0.99901 -0.06760 1 1;
28 154.00 1.01881 0.03360 1 1;
29 154.00 1.02039 0.08452 1 1;
30 154.00 1.04750 0.00523 1 1;
31 154.00 0.98200 0.00000 1 1;
32 154.00 0.98310 0.09363 1 1;
33 154.00 0.99720 0.17821 1 1;
34 154.00 1.01230 0.14993 1 1;
35 154.00 1.04930 0.17463 1 1;
36 154.00 1.06350 0.22379 1 1;
37 154.00 1.02780 0.10763 1 1;
38 154.00 1.02650 0.20808 1 1;
39 154.00 1.03000 -0.10395 1 1;
40 154.00 1.06024 0.19345 1 1;
41 154.00 1.02512 0.49660 1 1;
];
```

```
SW.con = [ ...
31 100 154.00 0.98200 0 4.00000 -1.00000 1.10000 0.90000 3.78530 1];


PV.con = [ ...
30 100.00 154.00 2.50000 1.04750 6.00000 -1.00000 1.10000 0.90000
1;
32 100.00 154.00 6.50000 0.98310 6.00000 -1.00000 1.10000 0.90000
1;
33 100.00 154.00 6.32000 0.99720 4.00000 -1.00000 1.10000 0.90000
1;
34 100.00 154.00 5.08000 1.01230 4.00000 -1.00000 1.10000 0.90000
1;
35 100.00 154.00 6.50000 1.04930 6.00000 -1.00000 1.10000 0.90000
1;
36 100.00 154.00 5.60000 1.06350 4.00000 -1.00000 1.10000 0.90000
1;
37 100.00 154.00 5.40000 1.02780 4.00000 -1.00000 1.10000 0.90000
1;
38 100.00 154.00 8.30000 1.02650 6.00000 0.00000 1.10000 0.90000 1;
39 100.00 154.00 10.00000 1.03000 6.00000 0.00000 1.10000 0.90000
1;
40 100.00 154.00 1.00000 1.00000 0.00000 0.00000 1.10000 0.90000 1;
41 100.00 154.00 1.00000 1.00000 0.00000 0.00000 1.10000 0.90000 1;
];


Supply.con = [ ...
30 100.00 0 3.00000 0.20000 0 100.00000 10.00000 0.01000 0 0 0 0 0;
31 100.00 0 10.00000 0.20000 0 100.00000 10.00000 0.01000 0 0 0 0
0;
32 100.00 0 7.00000 0.20000 0 100.00000 10.00000 0.01000 0 0 0 0 0;
33 100.00 0 7.00000 0.20000 0 100.00000 10.00000 0.01000 0 0 0 0 0;
34 100.00 0 6.00000 0.20000 0 100.00000 10.00000 0.01000 0 0 0 0 0;
35 100.00 0 7.50000 0.20000 0 100.00000 10.00000 0.01000 0 0 0 0 0;
36 100.00 0 6.00000 0.20000 0 100.00000 10.00000 0.01000 0 0 0 0 0;
```

```
37 100.00 0 6.00000 0.20000 0 100.00000 10.00000 0.01000 0 0 0 0 0;
38 100.00 0 9.00000 0.20000 0 100.00000 10.00000 0.01000 0 0 0 0 0;
39 100.00 0 10.00000 0.20000 0 100.00000 10.00000 0.01000 0 0 0 0
0;
40 100.00 0 10.00000 0.00000 0 100.00000 10.00000 0.01000 0 0 0 0
0;
41 100.00 0 10.00000 0.00000 0 100.00000 10.00000 0.01000 0 0 0 0
0;
];


PQ.con = [ ...
3 100 154.00 3.22000 0.02400 1.10000 0.90000 0;
4 100 154.00 5.00000 1.84000 1.10000 0.90000 0;
7 100 154.00 2.33800 0.84000 1.10000 0.90000 0;
8 100 154.00 5.22000 1.76000 1.10000 0.90000 0;
12 100 154.00 0.07500 0.88000 1.10000 0.90000 0;
15 100 154.00 3.20000 1.53000 1.10000 0.90000 0;
16 100 154.00 3.29000 0.32300 1.10000 0.90000 0;
18 100 154.00 1.58000 0.30000 1.10000 0.90000 0;
20 100 154.00 6.28000 1.03000 1.10000 0.90000 0;
21 100 154.00 2.74000 1.15000 1.10000 0.90000 0;
23 100 154.00 2.47500 0.84600 1.10000 0.90000 0;
24 100 154.00 3.08600 -0.92200 1.10000 0.90000 0;
25 100 154.00 2.24000 0.47200 1.10000 0.90000 0;
26 100 154.00 1.39000 0.17000 1.10000 0.90000 0;
27 100 154.00 2.81000 0.75500 1.10000 0.90000 0;
28 100 154.00 2.06000 0.27600 1.10000 0.90000 0;
29 100 154.00 2.83500 0.26900 1.10000 0.90000 0;
31 100 154.00 0.09200 0.04600 1.10000 0.90000 0;
39 100 154.00 11.04000 2.50000 1.10000 0.90000 0;
];


Line.con = [ ...
1 2 100 154.00 60 0 1.0000 0.00350 0.04110 0.69870 1.00000 0.00000
```

```
2.312 0.000 0.000 1;
1 39 100 154.00 60 0 1.0000 0.00100 0.02500 0.75000 1.00000 0.00000
2.311 0.000 0.000 1;
2 3 100 154.00 60 0 1.0000 0.00130 0.01510 0.25720 1.00000 0.00000
9.104 0.000 0.000 1;
2 25 100 154.00 60 0 1.0000 0.00700 0.00860 0.14600 1.00000 0.00000
4.463 0.000 0.000 1;
2 30 100 154.00 60 0 1.0000 0.00000 0.01810 0.00000 1.00000 0.00000
7.513 0.000 0.000 1;
3 4 100 154.00 60 0 1.0000 0.00130 0.02130 0.22140 1.00000 0.00000
2.642 0.000 0.000 1;
3 18 100 154.00 60 0 1.0000 0.00110 0.01330 0.21380 1.00000 0.00000
1.308 0.000 0.000 1;
4 5 100 154.00 60 0 1.0000 0.00080 0.01280 0.13420 1.00000 0.00000
4.931 0.000 0.000 1;
4 14 100 154.00 60 0 1.0000 0.00080 0.01290 0.13820 1.00000 0.00000
4.660 0.000 0.000 1;
5 6 100 154.00 60 0 1.0000 0.00020 0.00260 0.04340 1.00000 0.00000
9.098 0.000 0.000 1;
5 8 100 154.00 60 0 1.0000 0.00080 0.01120 0.14760 1.00000 0.00000
5.850 0.000 0.000 1;
6 7 100 154.00 60 0 1.0000 0.00060 0.00920 0.11300 1.00000 0.00000
7.940 0.000 0.000 1;
6 11 100 154.00 60 0 1.0000 0.00070 0.00820 0.13890 1.00000 0.00000
7.994 0.000 0.000 1;
6 31 100 154.00 60 0 1.0000 0.00000 0.02500 0.00000 1.00000 0.00000
12.136 0.000 0.000 1;
7 8 100 154.00 60 0 1.0000 0.00040 0.00460 0.07800 1.00000 0.00000
3.286 0.000 0.000 1;
8 9 100 154.00 60 0 1.0000 0.00230 0.03630 0.38040 1.00000 0.00000
2.743 0.000 0.000 1;
9 39 100 154.00 60 0 1.0000 0.00100 0.02500 1.20000 1.00000 0.00000
2.651 0.000 0.000 1;
10 11 100 154.00 60 0 1.0000 0.00040 0.00430 0.07290 1.00000 0.00000
5.510 0.000 0.000 1;
10 13 100 154.00 60 0 1.0000 0.00040 0.00430 0.07290 1.00000 0.00000
6.217 0.000 0.000 1;
```

```
10 32 100 154.00 60 0 1.0000 0.00000 0.02000 0.00000 1.00000 0.00000
10.786 0.000 0.000 1;
11 12 100 154.00 60 0 1.0000 0.00160 0.04350 0.00000 1.00000 0.00000
0.817 0.000 0.000 1;
12 13 100 154.00 60 0 1.0000 0.00160 0.04350 0.00000 1.00000 0.00000
0.886 0.000 0.000 1;
13 14 100 154.00 60 0 1.0000 0.00090 0.01010 0.17230 1.00000 0.00000
6.223 0.000 0.000 1;
14 15 100 154.00 60 0 1.0000 0.00180 0.02170 0.36600 1.00000 0.00000
2.671 0.000 0.000 1;
15 16 100 154.00 60 0 1.0000 0.00090 0.00940 0.17100 1.00000 0.00000
4.682 0.000 0.000 1;
16 17 100 154.00 60 0 1.0000 0.00070 0.00890 0.13420 1.00000 0.00000
3.073 0.000 0.000 1;
16 19 100 154.00 60 0 1.0000 0.00160 0.01950 0.30400 1.00000 0.00000
6.620 0.000 0.000 1;
16 21 100 154.00 60 0 1.0000 0.00080 0.01350 0.25480 1.00000 0.00000
4.586 0.000 0.000 1;
16 24 100 154.00 60 0 1.0000 0.00030 0.00590 0.06800 1.00000 0.00000
0.626 0.000 0.000 1;
17 18 100 154.00 60 0 1.0000 0.00070 0.00820 0.13190 1.00000 0.00000
3.007 0.000 0.000 1;
17 27 100 154.00 60 0 1.0000 0.00130 0.01730 0.32160 1.00000 0.00000
1.459 0.000 0.000 1;
19 20 100 154.00 60 0 1.0000 0.00070 0.01380 0.00000 1.00000 0.00000
3.866 0.000 0.000 1;
19 33 100 154.00 60 0 1.0000 0.00070 0.01420 0.00000 1.00000 0.00000
9.897 0.000 0.000 1;
20 34 100 154.00 60 0 1.0000 0.00090 0.01800 0.00000 1.00000 0.00000
7.911 0.000 0.000 1;
21 22 100 154.00 60 0 1.0000 0.00080 0.01400 0.25650 1.00000 0.00000
9.424 0.000 0.000 1;
22 23 100 154.00 60 0 1.0000 0.00060 0.00960 0.18460 1.00000 0.00000
0.982 0.000 0.000 1;
22 35 100 154.00 60 0 1.0000 0.00000 0.01430 0.00000 1.00000 0.00000
10.268 0.000 0.000 1;
23 24 100 154.00 60 0 1.0000 0.00220 0.03500 0.36100 1.00000 0.00000
```

```
5.334 0.000 0.000 1;
23 36 100 154.00 60 0 1.0000 0.00050 0.02720 0.00000 1.00000 0.00000
8.776 0.000 0.000 1;
25 26 100 154.00 60 0 1.0000 0.00320 0.03230 0.51300 1.00000 0.00000
2.536 0.000 0.000 1;
25 37 100 154.00 60 0 1.0000 0.00060 0.02320 0.00000 1.00000 0.00000
9.452 0.000 0.000 1;
26 27 100 154.00 60 0 1.0000 0.00140 0.01470 0.23960 1.00000 0.00000
4.556 0.000 0.000 1;
26 28 100 154.00 60 0 1.0000 0.00430 0.04740 0.78020 1.00000 0.00000
1.813 0.000 0.000 1;
26 29 100 154.00 60 0 1.0000 0.00570 0.06250 1.02900 1.00000 0.00000
2.697 0.000 0.000 1;
28 29 100 154.00 60 0 1.0000 0.00140 0.01510 0.24900 1.00000 0.00000
5.431 0.000 0.000 1;
29 38 100 154.00 60 0 1.0000 0.00080 0.01560 0.00000 1.00000 0.00000
13.032 0.000 0.000 1;
33 41 100 154.00 60 0 1.0000 0.10000 0.40000 0.00000 1.00000 0.00000
0.000 0.000 0.000 1;
39 40 100 154.00 60 0 1.0000 0.10000 0.40000 0.00000 1.00000 0.00000
0.000 0.000 0.000 1;
];


Bus.names =  ...
'1'; '2'; '3'; '4'; '5';
'6'; '7'; '8'; '9'; '10';
'11'; '12'; '13'; '14'; '15';
'16'; '17'; '18'; '19'; '20';
'21'; '22'; '23'; '24'; '25';
'26'; '27'; '28'; '29'; '30';
'31'; '32'; '33'; '34'; '35';
'36'; '37'; '38'; '39'; '40';
'41';
```

Index

Bibliography

[1] Power delivery & utilization update. Technical report, Electric Power Research Institute, March 2008.

[2] 2008 state of the market report, March 2009.

[3] World wind energy report 2010. Technical report, World Wind Energy Association, October - November 2010.

[4] T. Ackermann. *Wind Power in Power Systems*. Wiley, Hoboken, NJ, 2005.

[5] V. Ajjarapu and C. Christy. The continuation power flow: a tool for steady state voltage stability analysis. *Power Systems, IEEE Transactions on*, 7(1):416 –423, February 1992.

[6] R.N. Allan, A.M. Leite da Silva, and R.C. Burchett. Evaluation methods and accuracy in probabilistic load flow solutions. *Power Apparatus and Systems, IEEE Transactions on*, PAS-100(5):2539 –2546, May 1981.

[7] R. Baldick. *Applied Optimization: Formulation and Algorithms for Engineering Systems*. Cambridge, U.K.: Cambridge Univ. Press,, 2006.

[8] J. Bastian, Jinxiang Zhu, V. Banunarayanan, and R. Mukerji. Forecasting energy prices in a competitive market. *Computer Applications in*

Power, IEEE, 12(3):40 –45, July 1999.

[9] B. Borkowska. Probabilistic load flow. *Power Apparatus and Systems, IEEE Transactions on*, PAS-93(3):752 –759, May 1974.

[10] Claudio Canizares. Voltage stability assessment: concepts, practices and tools. Technical report, Electrical and Computer Engineering, University of Waterloo, 2002.

[11] Hsiao-Dong Chiang, Cheng-Shan Wang, and A.J. Flueck. Look-ahead voltage and load margin contingency selection functions for large-scale power systems. *Power Systems, IEEE Transactions on*, 12(1):173 –180, February 1997.

[12] A. Conejo and M.J. Aguilar. Secondary voltage control: nonlinear selection of pilot buses, design of an optimal control law, and simulation results. *Generation, Transmission and Distribution, IEE Proceedings-*, 145(1):77 –81, January 1998.

[13] D. Corbus, D. Lew, G. Jordan, W. Winters, F. Van Hull, J. Manobianco, and B. Zavadil. Up with wind. *Power and Energy Magazine, IEEE*, 7(6):36 –46, November-December 2009.

[14] S. Corsi, M. Pozzi, C. Sabelli, and A. Serrani. The coordinated automatic voltage control of the italian transmission grid-part i: reasons of the choice and overview of the consolidated hierarchical system. *Power Systems, IEEE Transactions on*, 19(4):1723 – 1732, November 2004.

[15] S. Corsi, M. Pozzi, M. Sforna, and G. Dell'Olio. The coordinated automatic voltage control of the italian transmission grid-part ii: control apparatuses and field performance of the consolidated hierarchical system. *Power Systems, IEEE Transactions on*, 19(4):1733 – 1741, November 2004.

[16] T. Van Cutsem and C. Vournas. *Voltage Stability of Electric Power Systems*. Kluwer, Norwell, MA, 1998.

[17] S. Grijalva and A.M. Visnesky. The effect of generation on network security: spatial representation, metrics, and policy. *Power Systems, IEEE Transactions on*, 21(3):1388 –1395, August 2006.

[18] S. Grijalva and Jr. Visnesky, A.M. Spatial representation of the effect of new generation on network security. In *Power Systems Conference and Exposition, 2004. IEEE PES*, pages 144 – 149 vol.1, October 2004.

[19] Santiago Grijalva, Scott R. Dahman, Kollin J. Patten, and Jr. Anthony M. Visnesky. Large-scale integration of wind generation including network temporal security analysis. *Energy Conversion, IEEE Transactions on*, 22(1):181 –188, March 2007.

[20] G. Hamoud and I. Bradley. Assessment of transmission congestion cost and locational marginal pricing in a competitive electricity market. *Power Systems, IEEE Transactions on*, 19(2):769 – 775, May 2004.

[21] Mike Heinrich. Renewble energy integration: Grid reliability impacts and solutions. Technical report, Electric Power Research Institute, July 2008.

[22] L. Holdsworth, X.G. Wu, J.B. Ekanayake, and N. Jenkins. Comparison of fixed speed and doubly-fed induction wind turbines during power system disturbances. *Generation, Transmission and Distribution, IEE Proceedings-*, 150(3):343 – 352, May 2003.

[23] P. Kundur, J. Paserba, V. Ajjarapu, G. Andersson, A. Bose, C. Canizares, N. Hatziargyriou, D. Hill, A. Stankovic, C. Taylor, T. Van Cutsem, and V. Vittal. Definition and classification of power system stability ieee/cigre joint task force on stability terms and definitions. *Power Systems, IEEE Transactions on*, 19(3):1387 – 1401, August 2004.

[24] P. Lagonotte, J.C. Sabonnadiere, J.-Y. Leost, and J.-P. Paul. Structural analysis of the electrical system: application to secondary voltage control in france. *Power Systems, IEEE Transactions on*, 4(2):479 –486, May 1989.

[25] T. Lakkaraju and A. Feliachi. Selection of pilot buses for var support considering n-1 contingency criteria. In *Power Systems Conference and Exposition, 2006. PSCE '06. 2006 IEEE PES*, pages 1513 –1517, 29 2006-November 1 2006.

[26] Stephen Lee. Critical operating constraints forecasting, a decision support tool. Technical report, Electric Power Research Institute, March

2008.

[27] F. Milano. An open source power system analysis toolbox. *Power Systems, IEEE Transactions on*, 20(3):1199 – 1206, aug. 2005.

[28] Federico Milano. *Pricing System Security in Electricity Market Models with Inclusion of Voltage Stability Constraints*. PhD thesis, University of Genova, Genova, Italy, April 2003.

[29] Liang Min, S.T. Lee, Pei Zhang, V. Rose, and J. Cole. Short-term probabilistic transmission congestion forecasting. In *Electric Utility Deregulation and Restructuring and Power Technologies, 2008. DRPT 2008. Third International Conference on*, pages 764 –770, April 2008.

[30] R. Piwko, D. Osborn, R. Gramlich, G. Jordan, D. Hawkins, and K. Porter. Wind energy delivery issues [transmission planning and competitive electricity market operation]. *Power and Energy Magazine, IEEE*, 3(6):47 – 56, November - December 2005.

[31] J.L. Sancha, J.L. Fernandez, A. Cortes, and J.T. Abarca. Secondary voltage control: analysis, solutions and simulation results for the spanish transmission system. In *Power Industry Computer Application Conference, 1995. Conference Proceedings., 1995 IEEE*, pages 27 –32, May 1995.

[32] R. Seydel. *Practical Bifurcation and Stability Analysis: From Equilibrium to Chaos*. Springer-Verlag, New York, second edition edition, 1994.

[33] J.C. Smith, M.R. Milligan, E.A. DeMeo, and B. Parsons. Utility wind integration and operating impact state of the art. *Power Systems, IEEE Transactions on*, 22(3):900 –908, August 2007.

[34] Liang Min Stephen Lee. Critical operating constrints & probabilistic congestion forecasting. Technical report, Electric Power Research Institute, September 2008.

[35] A. Vergnol, V. Rious, J. Sprooten, B. Robyns, and J. Deuse. Integration of renewable energy in the european power grid: Market mechanism for congestion management. In *Energy Market (EEM), 2010 7th International Conference on the European*, pages 1 –6, June 2010.

[36] Guoqiang Zhang, Boming Zhang, Hongbin Sun, and Wenchuan Wu. Ultra-short term probabilistic transmission congestion forecasting considering wind power integration. In *Advances in Power System Control, Operation and Management (APSCOM 2009), 8th International Conference on*, pages 1 –6, November 2009.

Vita

Han Kang was born in Seoul, Republic of Korea on 12 Mar 1984, the son of Kwangil Kang and Chunok Kim. He received the Bachelor of Science degree in Engineering from the Dongguk University in 2009. He applied to the University of Texas at Austin for enrollment in their engineering program. He was accepted and started graduate studies in August, 2009.

Permanent address: 5230 Thunder Creek Rd #125
Austin, Texas 78759

This thesis was typeset with LaTeX[†] by the author.

[†]LaTeX is a document preparation system developed by Leslie Lamport as a special version of Donald Knuth's TeX Program.